

The Surface Activity And Rheological Changes Induced In Lung Surfactant Resulting From Ozone Exposure

Justin W. Conway

A Thesis
in
The Department
of
Chemistry and Biochemistry

Presented in Partial Fulfillment of the Requirements
for the Degree of Master Science (Chemistry) at
Concordia University
Montréal, Québec, Canada

December 2009

© Justin W. Conway, 2009



Library and Archives
Canada

Published Heritage
Branch

395 Wellington Street
Ottawa ON K1A 0N4
Canada

Bibliothèque et
Archives Canada

Direction du
Patrimoine de l'édition

395, rue Wellington
Ottawa ON K1A 0N4
Canada

Your file *Votre référence*
ISBN: 978-0-494-67093-4
Our file *Notre référence*
ISBN: 978-0-494-67093-4

NOTICE:

The author has granted a non-exclusive license allowing Library and Archives Canada to reproduce, publish, archive, preserve, conserve, communicate to the public by telecommunication or on the Internet, loan, distribute and sell theses worldwide, for commercial or non-commercial purposes, in microform, paper, electronic and/or any other formats.

The author retains copyright ownership and moral rights in this thesis. Neither the thesis nor substantial extracts from it may be printed or otherwise reproduced without the author's permission.

In compliance with the Canadian Privacy Act some supporting forms may have been removed from this thesis.

While these forms may be included in the document page count, their removal does not represent any loss of content from the thesis.

AVIS:

L'auteur a accordé une licence non exclusive permettant à la Bibliothèque et Archives Canada de reproduire, publier, archiver, sauvegarder, conserver, transmettre au public par télécommunication ou par l'Internet, prêter, distribuer et vendre des thèses partout dans le monde, à des fins commerciales ou autres, sur support microforme, papier, électronique et/ou autres formats.

L'auteur conserve la propriété du droit d'auteur et des droits moraux qui protègent cette thèse. Ni la thèse ni des extraits substantiels de celle-ci ne doivent être imprimés ou autrement reproduits sans son autorisation.

Conformément à la loi canadienne sur la protection de la vie privée, quelques formulaires secondaires ont été enlevés de cette thèse.

Bien que ces formulaires aient inclus dans la pagination, il n'y aura aucun contenu manquant.


Canada

ABSTRACT

The Surface Activity And Rheological Changes Induced In Lung Surfactant Resulting From Ozone Exposure

Justin W. Conway

Lung surfactant is a complex mixture of phospholipids and membrane proteins that is located on the surface of alveoli within our lungs. Lung surfactant reduces the work associated with respiration and prevents the collapse of the alveoli sacs during breathing. The function of lung surfactant depends on lipid and membrane protein biophysical interactions which may be affected by the quality of air an individual inhales. Presently there exists extensive data concerning the chemical changes ozone, a major oxidant in photochemical smog, induces within exposed lung surfactant components. There is however little research focused on the biophysical impacts of lung surfactant oxidation. This research examines the surface activity, film morphology and rheological changes induced in model lung surfactant films by ozone exposure. These experiments will use monolayers as a model system to investigate film oxidation changes. The results of this research show that both unsaturated lipids and membrane proteins are ozone sensitive. The ozonolysis of films comprised of pure lipids and lipid-protein mixtures exhibit changes to surface activity, film organization and rheology. However, when membrane proteins are present the changes to film rheology after ozone exposure are not measurable. This thesis examines the molecular interactions that lead to these film property changes and relates them to lung surfactant physiological behavior.

Acknowledgements

As with most difficult works, the research presented here was only possibly because of the support team I had around me. I would like to thank my parents, my brother and sister, and Jessica for putting up with my ups and downs. I would also like to thank my supervisor and labmates who made my time during the M.Sc. a great experience.

Table of Contents

Chapter 1. Introduction	1
1.1. Lung Surfactant.....	1
1.1.1. Biological role of lung surfactant.....	1
1.1.2. Lung compliance and rheology.....	3
1.2. Tropospheric Ozone.....	5
1.2.1. Ozone exposure.....	5
1.2.2. Tropospheric Ozone Formation	6
1.3. Ozone and Respiratory Health	8
1.3.1. Ozonolysis of lung surfactant	8
1.3.2. Physiological response to ozone	9
1.3.3. Biophysical changes to oxidized lung surfactant.....	10
1.4. Lung Surfactant Composition and Physical Properties	11
1.4.1. Lung surfactant composition.....	11
1.4.2. Model lipid monolayers	12
1.4.3. Lung surfactant lipids	13
1.5. Lung Surfactant Proteins.....	14
1.5.1. Role of surfactant proteins SP-A and SP-D.....	14
1.5.2. Role of surfactant proteins SP-B and SP-C	15
1.6. Lung Surfactant Component Interactions	16
1.7. Literature Review.....	19
1.7.1. Lung surfactant rheology	19
1.7.2. Environmental pollution and lung surfactant surface properties	21

1.7.3. Existing therapeutic applications	22
Chapter 2. Research Objectives	24
2.1. Contributions of Authors	25
2.2. Lipid Structure and Rheology	25
2.3. Model Lung Surfactant Films of POPG and POPG/DPPC (20:80).....	26
2.4. Survanta Film Behavior	27
Chapter 3. A Rheological Comparison of Molecular Structure Effects in a Series of Phosphoglycerol and Phosphocholine Lipids	29
3.1. Abstract	29
3.2. Introduction.....	29
3.3. Methodology	33
3.4. Results and Discussion	35
3.5. Conclusion	46
Chapter 4. Surface Activity and Rheological Changes in Model Lung Surfactant Films Resulting from Ozone Exposure	48
4.1. Abstract	48
4.2. Introduction.....	48
4.3. Methodology	51
4.4. Results and Discussion	54
4.5. Conclusion	67
Chapter 5. Surface Activity and Rheological Changes in Survanta Films Resulting from Ozone Exposure	68
5.1. Abstract	68

5.2. Introduction.....	68
5.3. Methodology.....	73
5.4. Results and Discussion.....	76
5.5. Conclusion.....	90
Chapter 6. Conclusions.....	92
Chapter 7. References.....	97

Abbreviations

AFM:	atomic force microscopy
ADSA:	axisymmetric drop shape analysis
BAM:	Brewster angle microscopy
C:	condensed
CD:	circular dichroism
DO:	dioleoyl
DP:	dipalmitoyl
DOPC:	dioleoylphosphatidylcholine
DOPG:	dioleoylphosphatidylglycerol
DPPC:	dipalmitoylphosphatidylcholine
DPPE:	dipalmitoylphosphatidylethanolamine
DPPG:	dipalmitoylphosphatidylglycerol
ESI-MS:	electro-spray ionization mass spectroscopy
ETS:	environmental tobacco smoke
FM:	fluorescence microscopy
FTIR:	Fourier transform infrared spectroscopy
G:	gas
HPLC:	high performance liquid chromatography
LE:	liquid expanded
LS:	lung surfactant
LOP:	lipid ozonation products
MS:	mass spectroscopy

NMR:	nuclear magnetic resonance
NOX:	nitrogen oxides
PAN:	peroxyacetyl nitrate
PAT:	profile analysis tensiometer
PC:	phosphotidylcholine
PE:	phosphotidylethanolamine
PG:	phosphotidylglycerol
PO:	palmitoyloleoyl
POPC:	1-palmitoyl-2-oleyl-phosphotidylcholine
POPG:	1-palmitoyl-2-oleyl-phosphotidylglycerol
RDS:	respiratory distress syndrome
SP-A:	surfactant protein A
SP-B:	surfactant protein B
SP-C:	surfactant protein C
SP-D:	surfactant protein D
VOC:	volatile organic carbon
UV:	ultraviolet

List of figures

Figure 1.1. Schematic representation of monolayer surface pressure-area relationship on a pendant drop.....	4
Figure 1.2. General chemical reactions for tropospheric ozone formation.....	8
Figure 1.3. Schematic of lipid and surfactant protein interactions during respiration.....	18
Figure 3.1. PC and PG lipid structures	33
4.2. Reaction products for the surface ozonolysis of POPG monolayers	57
Figure 4.3. Isotherms of POPG and POPG/DPPC monolayers	58
Figure 4.4. Viscoelasticity of POPG, DPPC and POPG/DPPC monolayers	62
Figure 4.5. Viscoelasticity of POPG and POPG/DPPC monolayers	65
Figure 4.6. BAM images of POPG/DPPC monolayers	66
Figure 5.1. Ozonolysis of POPG and surfactant protein sequences.....	77
Figure 5.2. Real time changes to Survanta surface pressure during ozonolysis	78
Figure 5.3. Isotherms of POPG, DOPG, POPG/DPPC, and Survanta monolayers.....	80
Figure 5.4. Model protein images showing orientation within the lipid film	84
Figure 5.5. BAM images of Survanta monolayers.....	85
Figure 5.6. Recompressions of POPG, POPG/DPPC and Survanta monolayers	87
Figure 5.7. Rheological of Survanta, POPG/DPPC and POPG monolayers	89

List of equations

Equation (1)	2
--------------------	---

Chapter 1. Introduction

1.1. Lung Surfactant

1.1.1. Biological role of lung surfactant

As respiration occurs oxygen fills the lungs and crosses into the blood stream through a lipid membrane at the air-water interface¹⁻³. This interface is located in the lower lung airway at the surface of the alveolar sacs, which resemble small air bubbles covered in a thin film of phospholipids and membrane proteins. This film is termed lung surfactant (LS) and is secreted by type II epithelial cells. It serves to reduce the surface tension acting to collapse alveoli at the end of exhalation (termed atelectasis), and based on its composition is able to rapidly compress and expand over the alveolar surface⁴. Lung surfactant research was initially driven to understand and remedy respiratory health conditions such as infantile respiratory distress syndrome (RDS). A significant result of lung surfactant research was the creation of lung surfactant replacements that are routinely used to this day⁵.

Lung surfactant films reduce the surface tension at the surface of alveoli by preferentially adsorbing in the air-water interface; this behavior is due to the amphiphilic character of lipids. The collapsing surface tension force within alveoli arises because they are essentially air sacs located in a water medium. The surface tension of water is about 70 mN m^{-1} and acts to minimize the alveolar volume and collapse the bubble. Consequently, the surface tension also helps to regulate the expansion of alveoli as

respiration occurs; when alveoli are filled with air during inhalation, they increase in size causing the phospholipid lining to reach a more expanded state. As the size of the alveoli air pocket increases the surface tension acting to collapse it also increases. Alveoli which increase in size faster than others will therefore experience greater surface tension slowing their expansion⁶. The balance between gas pressure within the alveoli and the surface tension acting to collapse it is described by the Young-Laplace equation (Equation 1). Where P is the pressure (mN m⁻²), γ is the surface tension (mN m⁻¹) and R_x are the principle radii of curvature (m).

$$P = \gamma \left(\frac{1}{R_1} + \frac{1}{R_2} \right) \quad \text{Equation (1)}$$

Pulmonary surfactant must maintain reduced surface tension to prevent the collapse of alveoli as they inflate and deflate during respiration. The lowered surface tension of the alveolar sacs ensures that the lungs can be filled with minimal work since the pressure difference is kept low. The lung surfactant film must therefore have a composition which allows rapid compression and expansion over the surface of the alveoli as breathing occurs⁷⁻⁹. Flow properties of pulmonary surfactant films accommodate changes in alveolar volume and are described by a property termed lung compliance¹⁰. Optimal lung compliance refers to films that readily adjust to pressure changes during both inhalation and exhalation. A low compliance corresponds to a more rigid lung surfactant film which does not readily stretch and causes difficulty during inhalation. Alternatively, a high compliance results in a difficulty exhaling air from the lungs, which is associated with a loss of elasticity in the lung surfactant films and tissues. These medical conditions can be caused by emphysema and chronic coughing¹¹⁻¹³.

1.1.2. Lung compliance and rheology

Lung compliance is strongly dependent on the rheological behavior of lung surfactant films on the alveolar surface¹⁰. Lung compliance is regulated through a balance of viscosity and elasticity which respectively describe the flow and deformation of a material. Materials which contain both viscous and elastic components are said to be viscoelastic. The Maxwell model describes viscoelastic behavior as a two component system consisting of a dashpot and spring connected in series¹⁴⁻¹⁶. The dashpot and spring components correspond to the dissipation and conservation of energy as the system is stressed. As a stress is applied to a thin membrane, the force generates measurable flow and deformation properties. In lung surfactant films this corresponds to the alveolar volume oscillations during respiration. The alveolar oscillations cause surfactant films to flow, compress, and expand as breathing occurs. This can be likened to the stress felt in the material of a balloon as the volume is increased or decreased. The applied force experienced by lung surfactant films is a dilational stress generated by the alveolar expansion and compression. The lipids in the film are being displaced in plane at the surface with respect to their neighbor.

Dilational rheology measures the viscoelasticity of thin films by relating oscillations in the available surface area of a monolayer to a surface pressure response (Figure 1). Several groups have described the mathematical derivations (Appendix 1) required to relate surface area and pressure oscillations to both dilational viscosity and elasticity^{14,16,17}. The flow and recovery of the lipid film at the alveolar surface is dependent on its viscoelastic properties which are governed by the component chemical structure and consequent film organization. Although the rheological properties of a film

describe the behavior of the whole system, their strength originates from individual molecular interactions. Any chemical modification to individual lung surfactant components could alter the film viscoelasticity and affect the flow, compression and expansion of the system^{18,19}.

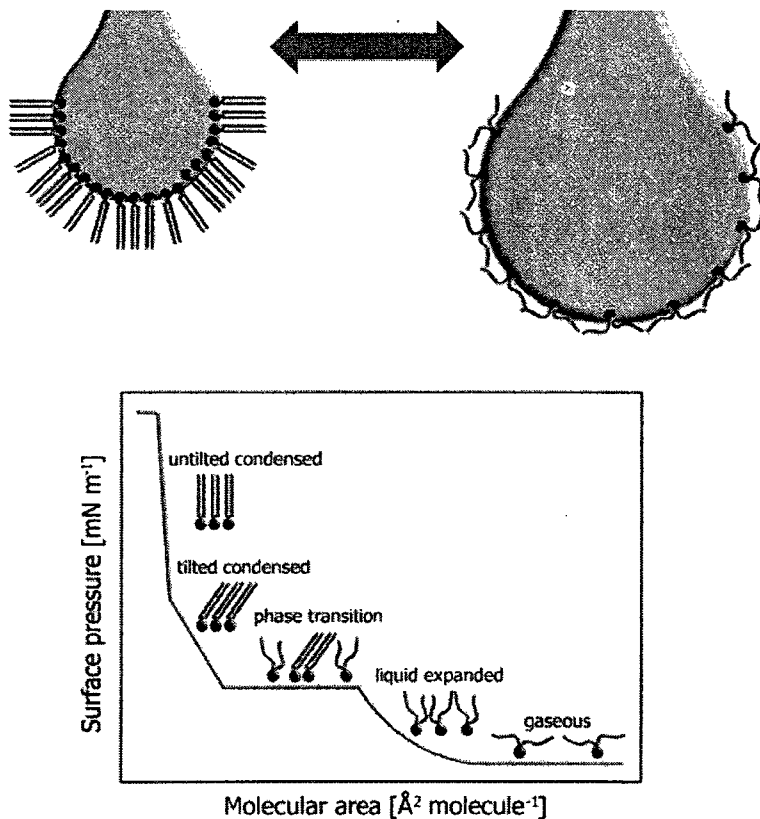


Figure 1.1. Schematic representation of lipid conformational changes during compression and expansion at the pendant drop surface during rheology measurements (top). Schematic representation of surface pressure-area relationships for a lipid monolayer (bottom).

1.2. Tropospheric Ozone

1.2.1. Ozone exposure

It is generally accepted that the lung surfactant system functions through a dynamic interplay between both lipid and protein components^{3,8}. The reduction in surface tension and the ability to rapidly accommodate alveolar volume changes is achieved through specific combinations of saturated and unsaturated phospholipids interacting with lung surfactant proteins. Reactive chemical species which are inhaled through the lung surfactant film may react with both lipid and protein components^{11, 13, 20}. One example of a commonly inhaled airborne chemical is ozone. Ozone inhalation is known to create respiratory complications and is readily found in certain densely populated areas.

Environmental respiratory health hazards such as photochemical smog include ozone as the main oxidant component²¹⁻²³. Ozone is a powerful oxidizing agent normally found in a concentrated gaseous layer in the stratosphere. Ozone formation in the troposphere is in most cases is a result of anthropogenic activities and is considered a harmful pollutant^{24, 25}. Economic growth in agricultural and industrial domains has led to significant concentrations of low lying ozone, as well as other gaseous pollutants. The main precursors of these primary pollutants originate from the combustion of fossil fuels for energy, which releases volatile organic compounds (VOCs) and nitrogen oxides (NOXs). Agricultural activities such as dairy farming are also a significant source of tropospheric ozone precursors in some countries. Some reports have identified the emissions of cattle defecation as the second largest contributor to photochemical smog in certain regions^{23, 26}.

Ozone was first detected in photochemical smog during the 1940s in the Los Angeles basin and has subsequently been found in air pollution in most industrialized cities worldwide¹². Smog describes air pollution containing a mixture of nitrogen oxides (NOX), halogenated and volatile organic compounds (VOC), peroxyacetyl nitrate (PAN) as well as ozone, all of which are harmful to the respiratory system as they are notably reactive and will chemically modify lung surfactant films¹³. The formation of these highly reactive compounds requires the presence of sufficient UV radiation. As the ozone layer gradually becomes thinner and fills with holes, increasing amounts of UV radiation will reach the earth and the potential for ozone and photochemical smog formation will increase.

1.2.2. Tropospheric Ozone Formation

In the presence of sufficient photolytic energy gaseous pollutants can react to form a complex mixture of airborne chemical species. The resulting complex mixture is due to the large number of atmospheric chemicals available and their varying chemical reaction pathways. The complex series of reactions that generate ozone and other photochemical smog components include both radical and heterogenous mechanisms²¹. A summary of these reactions can be seen in Figure 1. 2. Generally, ozone formation is governed by the concentrations of NOXs, VOCs in the form of methane or peroxy radicals ($\text{HO}_2\cdot$, $\text{RO}_2\cdot$), hydroxy radicals ($\text{HO}\cdot$), as well as existing ozone and available photolytic energy. The first step in the formation of ozone depends on the availability of hydroxyl radicals. Sources of hydroxyl radicals include aldehydes and peroxides, but the greatest contribution comes from the photolytic cleavage of existing ozone ($\lambda = 330 \text{ nm}$). The photolytic cleavage of ozone generates oxygen and an excited state oxygen atom

which reacts with available water vapor to form hydroxyl radicals. In the next step hydroxyl radical species react with CO and VOCs to form peroxy radical molecules ($\text{HO}_2\cdot$, $\text{RO}_2\cdot$). The organic peroxy radicals ($\text{RO}_2\cdot$) can react through an oxygen subtraction reaction with NO to yield $\text{RO}\cdot$, which readily reacts with oxygen to form ($\text{HO}_2\cdot$). Limiting NOX concentrations are also a key component for ozone forming chemical pathways. In clean air conditions where NOX concentrations are less than 50 parts per thousand (ppt) the peroxy radical reacts with existing ozone generating a hydroxyl radical and oxygen. When NOX concentrations exceed 100 ppt hydroxyl radicals react with available NO to generate NO_2 . Exposure to sufficient UV radiation ($\lambda = 420 \text{ nm}$) initiates the dissociation of one excited state oxygen atom from NO_2 , which rapidly combines with available oxygen to form ozone. The reaction scheme presented here is a simplified overall picture of reactions leading to ozone formation. The atmospheric chemistry that occurs involves many inter-conversions and feedback loops between available chemical species as well as the influence of light and temperature (i.e. daytime or night time).

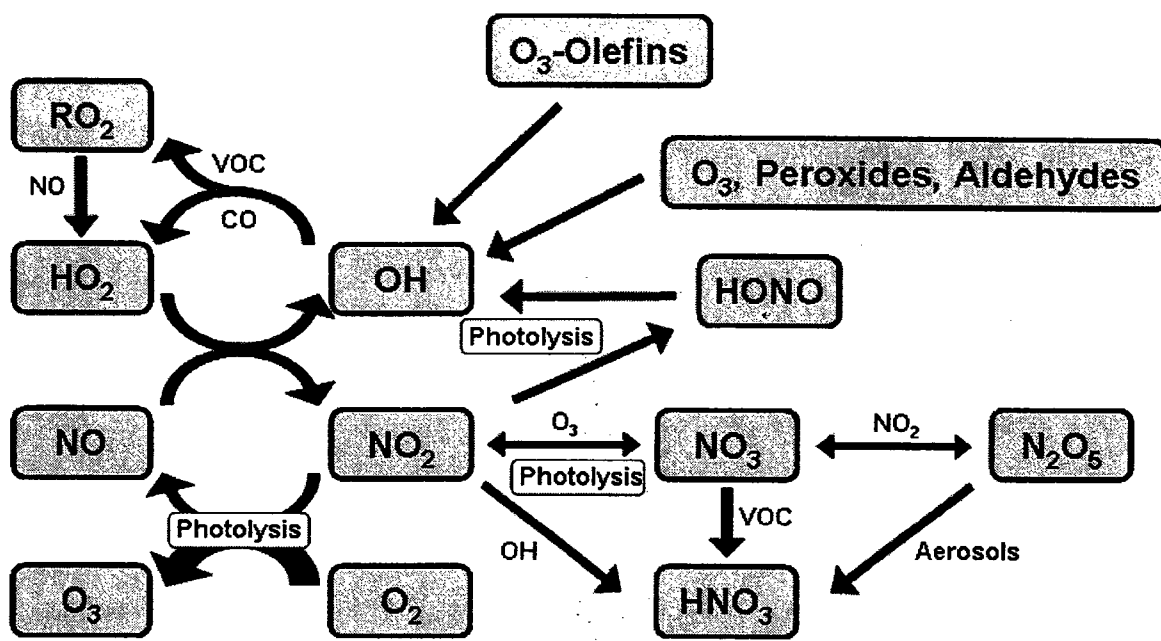


Figure 1. 2. General chemical reactions that lead to tropospheric ozone formation (modified from²¹).

1.3. Ozone and Respiratory Health

1.3.1. Ozonolysis of lung surfactant

Lung surfactant is composed of a mixture of saturated/unsaturated lipids and membrane proteins. Ozone will react with the unsaturated phospholipid and sensitive protein components within lung surfactant films, thereby changing their chemical structure, surface behavior and releasing a cascade of toxic oxidation products^{20, 27}. Lung lining fluids contain lipids and fatty acids that generally have between 20-40% unsaturation within the alkyl chains^{28,29}. Unsaturated units are cleaved through the Criegee mechanism which yields aldehyde, carboxylic acid and hydroxyl hydroperoxide moieties at the point of cleavage^{30,31}. The reaction proceeds through an unstable intermediate termed the Criegee ozonide which degrades into the corresponding

functionalities. Membrane proteins with ozone sensitive residues such as cysteine, methionine, tryptophan and tyrosine are also known to be chemically modified in different ways^{18,27}. These targets represent the precursors for the vehicles of ozone toxicity into deeper tissues. Due to the high reactivity of ozone, it is not able to penetrate deeply into other tissues beyond the lower lung airways. The primary oxidation reaction will occur at the air-water interface within the lining of the lung, a situation termed reactive adsorption^{32,33}. It is the secondary reaction products that will penetrate into deeper regions of the respiratory tract and cause inflammation. Significant research has gone into the investigation of how ozone toxicity is translated through the lung surfactant membrane^{12,34}. Very little work has investigated how lung surfactant surface properties change after ozone exposure³⁵.

1.3.2. Physiological response to ozone

Inhalation of ozone has been shown to cause airway inflammation, coughing, shortness of breath, or even increased susceptibility to bacterial infection³⁶⁻³⁹. These respiratory health issues arise from the fact that ozone can react with the phospholipid lining of the lung airways and lung surfactant at the alveolar surface. Respiratory effects of ozone inhalation have been documented as early as 1957-58⁵. Since the cells lining the airways are continually replaced the body can repair most short term ozone damage, however like any other health hazard long term exposure to ozone can lead to more permanent respiratory complications. The group most at risk from ozone exposure comprises individuals who spend a large amount of time outdoors. The risk is greatest during the summer when greater levels of UV radiation lead to increased photochemical smog formation. Individuals with chronic respiratory health problems such as asthma are

more sensitive to ozone inhalation. These higher risk groups will typically experience symptoms more rapidly, at lower exposure concentrations than healthy groups. Meteorological conditions and weather patterns have an influence on the environmental chemistry that occurs and forms photochemical smog as well as the concentrations and distribution of the pollutant products that may accumulate. In order to reduce the risk of ozone exposure, the government working with weather media stations has taken measures to inform the public when ozone concentrations become significantly dangerous. The information is generally listed as a color coded index and gives ozone exposure risks over a 24 hour day to day period with concentrations typically ranging 0 - 0.225 ppm.

Lipid ozonation products (LOPs) are the main reaction products as ozone is inhaled and have been associated with perpetuating oxidative stress. The LOPs that are thought to be responsible for transmitting ozone toxicity are mainly aldehyde and hydrogen peroxide products^{12,34}. It has been postulated that a cascade of LOPs act as secondary messengers transmitting ozone toxicity deeper within biological organisms^{13, 20,32}. The evolutionary reaction of the respiratory system to oxidative stress has been the development of defense mechanisms in the form of antioxidants such as uric acid, ascorbic acid, glutathione and vitamin E^{40,41}. Initially as ozone is inhaled it is consumed in reactions with the antioxidants in the upper airways. Once the sacrificial antioxidant defense is depleted the ozone reacts with the lipids and proteins in the lung lining fluids.

1.3.3. Biophysical changes to oxidized lung surfactant

Ozone damage is not limited to the physiological response to aldehydes, carboxylic acids and hydrogen peroxides, it also takes the form of decreased lung surfactant film properties, which is the focus of this research. Properties such as film

surface tension, fluidity and absorption exhibited by lung surfactant are essential for normal respiration. These biophysical properties are dependent on the chemical structure and resulting component interactions which are modified by oxidation^{18,19,35}. Many groups have investigated the surface behavior and morphology of the model lung surfactant films with the addition of lung surfactant proteins. The comparison of film surface properties, before and after direct exposure to ozone has to our knowledge not been reported. In this thesis we describe the consequences ozone exposure has on the surface activity, film morphology and dilational rheological properties of lung surfactant films.

1.4. Lung Surfactant Composition and Physical Properties

1.4.1. Lung surfactant composition

The biological function of lung surfactant requires a combination of several lipid characteristics to achieve optimal film properties. The high surface tension reduction needed at the alveolar surface to prevent collapse can only be achieved by a highly ordered saturated lipid film. The rapid compression and expansion of the lung surfactant film requires significant film fluidity, which can be increased through the incorporation of unsaturated lipids. Lung surfactant composition by weight is 90% phospholipids and 10% surfactant associated proteins^{28,29}. The major lipid components include up to 80% saturated phosphatidylcholine (PC), predominantly found as dipalmitoylphosphatidylcholine (DPPC), and 10% phosphatidylglycerol (PG) mainly found as 1-palmitoyl-2-oleyl-phosphatidylglycerol (POPG)⁷⁻⁹. The remaining 10%

corresponds to minor lipid components such as phosphatidic acid, phosphatidylinositol, phosphatidylethanolamine and cholesterol.

1.4.2. Model lipid monolayers

Lipid monolayers are used as model systems to study a variety of membrane properties including lung surfactant component behavior^{4,42-46}. Model monolayers are considered to be two dimensional systems whose molecular packing or phase behavior is described using three dimensional analogies^{47,48}. Three dimensional phase transitions classically involve the compression of atoms or molecules from a gaseous to liquid to solid state, generating an increasing amount of intermolecular interactions in the same transition order. Initially at high molecular areas the lipids in a monolayer are located far enough apart that there are no interactions between them. This is described as a gaseous phase. When the available molecular area is reduced lipid molecules begin to interact and a transition into a liquid expanded state is occurs. Upon further compression the molecules begin to line up and pack together in a coherent film termed a condensed phase. The compression of a monolayer effectively displaces an increasing number of water molecules from the interface thereby reducing the surface tension. Fully saturated alkyl chain tail groups have the greatest conformational flexibility and can pack most efficiently into a condensed phase thereby generating the greatest reductions in surface tension⁴⁷. Lipids that contain units of unsaturation in their side chains have a lowered packing ability which limits their film surface tension⁴⁷. When the molecular area available to lipids reaches its limit any further compression results in the monolayer collapse. In general, the collapse pressure of a monolayer decreases with limitations on molecular packing (*e.g.* units of unsaturation).

The molecular structures of the head group and side chains become increasingly important for packing efficiency during film compressions. As lipids are brought closer together the tail groups begin to interact through van der Waals forces and hydrophobic effects, which add cohesive strength to the monolayer⁴⁷. The length of the hydrophobic tail group is relevant in determining surface behavior⁴⁷. Head group interactions between lipids in general take the form of electrostatic or hydrogen bonding and may be disrupted or enhanced by ionic species and pH levels⁴⁷. For example charged lipid head groups effectively occupy greater amounts of space because of electrostatic repulsion. Membrane proteins in lung surfactant films orient themselves within the lipid film such that hydrophobic and hydrophilic structures are favorably interacting. Through these types of biophysical interactions a coherent multi-component film is maintained at the alveolar surface.

1.4.3. Lung surfactant lipids

DPPC, the main saturated phospholipid component of lung surfactant forms a condensed phase which reduces the surface tension to near zero values. The unsaturated POPG component forms a fluid liquid expanded (LE) phase associated with facilitating the rapid re-spreading of the film. A mixture of DPPC and POPG will combine both the surface tension reduction and film fluidity properties needed in functional lung surfactant. Lung surfactant is able to reduce the surface tension in the alveoli, rapidly spread and compress over their surface with respiration and decrease the work of breathing^{7, 8}. These properties are linked to the biophysical interactions of lipids and surfactant proteins with each other and the air-water interface. The surface behavior of lipids is determined by their hydrophobic alkyl side chains and hydrophilic polar head groups. The lung

surfactant proteins also exhibit an amphiphilic tertiary structure which is generated through their amino acid sequence. In an air-water medium such as the environment found surrounding lung surfactant, the amphiphilicity of components promotes their positioning at the interface and an ordered lung surfactant film is formed.

1.5. Lung Surfactant Proteins

The 10% surfactant proteins (SP) correspond to four specific types: SP-A, SP-B, SP-C, and SP-D; these proteins are secreted along with the phospholipids from type II alveolar cell^{49,50}. These four proteins can be classified into two groups, the hydrophilic proteins SP-A and SP-D and the hydrophobic proteins SP-B and SP-C. SP-A and SP-D have been observed to have a significant role in pulmonary innate immune systems through their interaction with specific pathogenic molecular patterns^{3,51}. The increased susceptibility to bacterial infection following ozone exposure may be linked to the oxidation of SP-A and SP-D which renders them non-functional⁵². These proteins have also been shown to participate in the regulation of inflammatory responses, phagocytosis and the production of reactive oxygen species following tissue injury.

1.5.1. Role of surfactant proteins SP-A and SP-D

SP-A has been shown to play a role in augmenting the phospholipid uptake and secretion by type II alveolar cells as well as possibly enhancing the surface activity of SP-B. Investigation into the biological significance of lung surfactant proteins has been performed using knock-out mice for each respective protein. It has been found that knock-out mice for both SP-A and SP-D have notable decreases in microbial or viral particle clearance as well as unregulated inflammatory responses³. However, only the

knock out SP-D mice exhibited significantly irregular lung morphology consisting of a foamy phospholipid-macrophage fluid and an enlarged alveoli space. In the case of SP-A, normal functionality can be restored through intratracheal dosing with supplemented SP-A. The role of SP-A and SP-D with respect to the pulmonary innate immune system includes research into viral infections, bacterial pneumonia, and cystic fibrosis. Individuals suffering from these conditions exhibit a marked decrease in both of these proteins^{53,54}.

1.5.2. Role of surfactant proteins SP-B and SP-C

The lung surfactant proteins SP-B and SP-C exhibit essential extracellular roles in normal respiratory physiology, by modifying phospholipid film organization as breathing occurs. The structures of SP-B and SP-C have been reported as a 17 kDa homodimer and a 21 kDa peptide respectively^{3,55}. There exists a significant amount of research showing that lung surfactant protein SP-B is linked to modifying lipid film organization and surface behavior^{4, 42-46}. SP-B has been reported to modify the collapse mechanism and subsequent reincorporation of unsaturated LE components to the interface during respiration⁴⁵. SP-B contains an overall positive charge that may cause it to preferentially interact with anionic lipids such as POPG^{46,55,56}. The secondary structure of SP-B has been examined with FTIR experiments which show that the protein contains between 27-45% amphiphilic helical structure that favors interactions with interfacial lipid films^{18,57,58}. SP-B has been shown to be critical for functional respiration in case studies of human and animal subjects. These studies found insufficient SP-B concentrations to be lethal⁵⁹.⁶⁰ Recently, a secondary role of SP-B has been suggested, in which it may possess

antimicrobial properties^{3,61}. This idea stems from the ability of SP-B to fuse lipid membranes which is also a mechanism used by antimicrobial peptides.

SP-C is an extremely hydrophobic peptide which has been noted to cause problems in its isolation and bio-synthesis. FTIR, CD, and NMR studies have shown that SP-C is predominantly helical in secondary structure³. The helical structure and extreme hydrophobicity is due to a valine rich sequence followed by a series of branched hydrophobic amino acids (Val, Ile and Leu). The SP-C structure also contains two positively charged residues and two palmitoylated cystein residues at the N-terminal of the protein which facilitates its interactions within lipid films. The extracellular activity that has been linked to SP-C is very similar to SP-B. SP-C has been shown to help stabilize lipid film organizations by maintaining collapsed material at the interface⁶². This facilitates re-spreading following film compression and increases adsorption of lipids to the air-water interface.

1.6. Lung Surfactant Component Interactions

Lung surfactant performance at the alveolar surface during respiration is linked to the cooperativity of the lipid-protein mixture^{4,42-46}. Figure 1.3 represents a simplified version of the interactions between lipids and a lung surfactant protein (SP-C) that occur during normal respiration. At the end of inhalation the alveoli are filled with air and have reached their greatest surface areas. This represents the maximum expanded state of the lung surfactant film (Figure 1.3 step 1). As exhalation begins the available surface area is reduced and the film begins to be compressed. The mixture of saturated and unsaturated lipid components are brought into closer proximity and their packing limitations become more pronounced (Figure 1.3 step 2). The saturated lipids begin to enter a condensed

phase at lower molecular areas while the unsaturated lipids remain in a liquid expanded state. This results in phase separation between the lipid components. As exhalation continues the liquid expanded material reaches a limiting molecular area and begins to collapse. This LE material is squeezed out of the interface into the water subphase (Figure 1.3 step 3)^{3,63}. It is during the squeeze out process that the role of the surfactant proteins becomes evident. The surfactant proteins SP-B and SP-C have been shown to strongly interact with the LE material and during the squeeze out and adjust their surface orientation to remain in contact with the collapsed material^{45,55,56}. At the end of exhalation (Figure 1.3 step 4) the surfactant proteins span the interfacial and expelled material and act as anchors which hold the squeezed out material near the interface as a surface associated reservoir⁶⁴. This leaves a DPPC-rich film at the surface which compresses to near zero surface tensions thereby reducing the work for breathing. Following this last step inhalation begins and proceeds through the reverse series of steps, the surfactant protein now facilitate the reincorporation of the collapsed material into the overlying film. Without the presence of surfactant proteins to modify the collapse event and anchor expelled material, collapsed unsaturated lipid components would be irreversibly lost to the subphase^{45,56,65}.

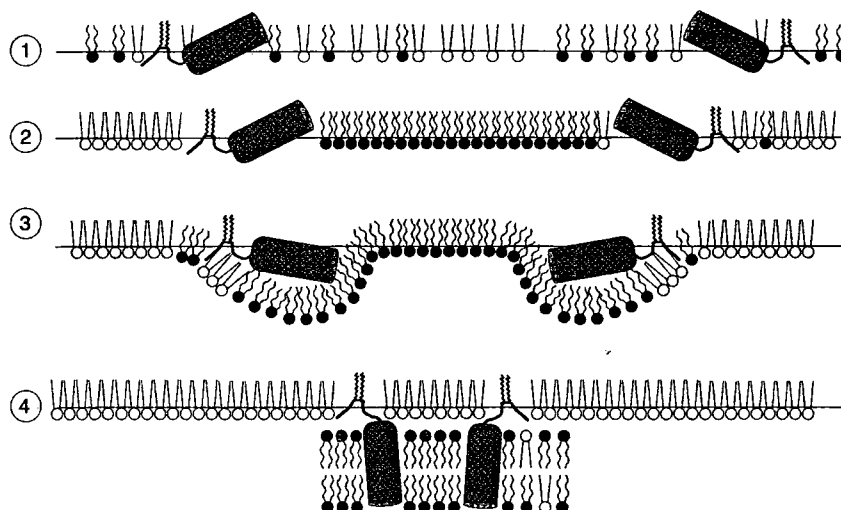


Figure 1.3. Schematic of lipid and surfactant protein interactions during respiration³.

Atomic force microscopy (AFM) experiments with different combinations of lipids and the surfactant proteins have confirmed the formation of these surface associated reservoirs^{4,42-46}. Measurements of height differences between phase separated material show that before the squeeze out pressure the condensed phase is higher than the LE phase material. Above the squeeze out pressure which corresponds to the collapse pressure of the LE phase, the LE material is now higher than the condensed phase. This height difference is attributed to the multilayer formation of LE material as it is squeezed out and held at the interface by the surfactant proteins. The squeezing out process allows monolayer films to fold and accommodate reduced molecular areas. The component phase separation and fold formation have been extensively observed using both Brewster angle microscopy (BAM) and fluorescence microscopy (FM)^{4,42-46}. BAM and FM images of this process show the disappearance of the folded structures and reincorporation of the LE phase material as a film is relaxed from compressed state. Additionally the fluidity of LE material contributes to the reincorporation of associated lipid reservoirs into the

interface during inhalation. The specific roles and functions of the various lipid and protein components are not fully understood and much of the research to date is focused on elucidating these mechanisms

1.7. Literature Review

1.7.1. Lung surfactant rheology

Previous research with respect to the individual roles of SP-B and SP-C initially concluded that SP-B serves the same function as SP-C with greater efficiency^{3, 4, 42-46}. However this perception is changing as their respective roles become distinguished using advances in technology and instrumentation. Alonso *et al*^{4, 42, 62, 66} have shown that SP-C plays an important role in the regulation of film viscosity during respiration. The viscosity of lung surfactant films must be regulated to oppose the existing surface tension gradient between the upper and lower lung airways. This gradient acts to drive the lung surfactant from a low surface tension at the alveoli surface (0-50 mN m⁻¹) towards the higher surface tension in the trachea (30 mN m⁻¹)⁶⁷ and connecting airways (15 mN m⁻¹)⁶⁸. The lowest surface tensions occur at the surface of the alveoli at the end of exhalation which also corresponds to the greatest surface tension gradient. Increased film viscosity during this period would minimize the flow of the film away from the alveoli surface. A function of SP-C appears to be the ability to organize the film in such a way that viscosity is maximized which prevents loss of lung surfactant. At the end of exhalation the film is in a compressed state which means that LE and condensed phase separation has occurred and that the LE material has been squeezed out and anchored by SP-B. Alonso *et al* suggest that the condensed phase domains which remain at the

interface generate high viscosities by jamming against each other as the surface tension gradient induces flow away from the alveoli surface. The work also proposes that SP-C holds collapsed LE material as multilayer patches between the condensed domains and because of its film spanning orientation links these multilayers to the overlying monolayer. Therefore a complete transition to condensed phase is not necessary to achieve high viscosity because of both of these effects^{4,42}.

The molecular packing within a monolayer determines the extent of intermolecular interactions which is directly related to rheological properties and lung compliance. As the lipid components are brought within closer proximity to each other the stabilizing interactions between neighboring lipids increases. Alternatively, as a compressed monolayer is relaxed the lipids re-spread over the surface and interactions decrease. Considering the dynamic conditions in which lung surfactant is located, these compression-expansion cycles require specific flow and deformation film properties described by viscosity and elasticity respectively.

The rheology of many of the lung surfactant components have been investigated using various techniques. These studies have focused on pure lipid films^{14,15,69,70} as well as multicomponent mixtures including both lipids and the surfactant proteins SP-B and SP-C^{65,71-73}. The incorporation of SP-B and SP-C in lipid films leads to a marked increase in the viscosity and elasticity compared to pure lipid monolayers. Single component research has shown that viscoelasticity strongly depends on the phase state of the film^{14,69,70}. Viscoelasticity increases with surface pressure and chain saturation as this maximizes tail interactions. Previous work has also shown that lipid films with LE-condensed (C) phase transitions will exhibit a significantly greater slope in viscoelasticity

following the transition¹⁴. However, during the phase transition there is no noted increase in the rheological properties. This is attributed to a constant pressure range during which the proportions of LE and C phase material are simply being interchanged^{69,70}. Although the effects of lipid side chain structures have been examined, very little information exists on the rheological differences generated by head group interactions. Available literature indicates that lipid-lipid and lipid-water head group interactions can generate marked differences in rheology¹⁵.

1.7.2. Environmental pollution and lung surfactant surface properties

Model lung surfactant films have been extensively investigated in terms of their phase transitions⁷²⁻⁷⁴ surface morphology^{43,56,75}, synthesis/secretion/reuptake⁷⁶, composition effects, temperature dependence⁷⁷ as well as mechanical properties⁷⁸⁻⁸⁰. Much of the original pioneering work⁵ revolved around the characterization of the lung surfactant behavior and clinical applications towards respiratory diseases.

The research discussed up to this point demonstrates that multiple components in lung surfactant films work together to achieve specific surface activity, morphology, and viscoelasticity. Very few papers have addressed how these parameters change when an individual inhales chemically reactive environmental substances. Work by Pryor *et al*^{20, 34} was some of the first addressing the chemical changes to lung surfactant components following the inhalation of tropospheric ozone. This work focused on how ozone toxicity is transmitted deeper into tissues. Salgo *et al*³⁵ used FM to investigate POPC film changes when exposed to ozone or when co-spread with the oxidation products. The oxidized components in the monolayer were noted to create an increased polar environment in the film which allowed greater water penetration into the film. This lead

to altered packing order, reduced interactions between acyl chains linked to increased membrane fluidity. Recent work investigating the effects of environmental tobacco smoke (ETS) which is also known to contain reactive free radicals and oxidizers, shows marked changes to lung surfactant mechanical behavior and morphology^{18,19}. Their findings indicate that the interaction of ETS components with lung surfactant mixtures leads to decreased maximum pressure and alters the distribution and fraction of condensed phase material. These changes combined with noted changes to the reversible collapse mechanism may lead to decreased rheological performance. Mass spectrometry (MS) results by Stenger *et al*¹⁸ of ETS exposed Survanta containing SP-B shows that aromatic residues are oxidized. FTIR measurements of SP-B and SP-C after ETS exposure exhibit significant changes to conformation which yields the altered surface activity and morphology. Similar research involving other anthropogenic pollution found that eicosane, a component of nanoparticles from diesel exhaust causes a decrease in the collapse pressure of DPPC films⁸¹.

1.7.3. Existing therapeutic applications

One direct application of this research is to develop lung surfactant replacement therapies for an array of respiratory diseases and environmental health hazards, the most common medicinal and environmental examples being infant RDS and inhalation of atmospheric oxidants, respectively. Successful clinical treatments for respiratory diseases include both synthetic pulmonary replacements, containing biomimetic peptides⁸² with purified lipids, as well as natural surfactant extracts from bovine lung lavages^{29, 83, 84}. Examples of naturally derived lung surfactant replacements include the Alveofact, Curosurf, and Suravanta (bovine derived). These therapeutic medications typically

involve the purification of the primary lung lavage to remove unwanted material. In the case of Survanta, extracts are treated to remove cholesterol as well as the SP-A and SP-D proteins. DPPC, palmitic acid and triacylglycerols are then supplemented to achieve a phospholipid concentration of near 25 mg/ml. Many pharmaceutical companies have also developed synthetic lung surfactant replacements which use synthetic peptides and a blend of lipids to achieve similar properties found in natural lung lavages. These include medications such as Exosurf, Pumactant, KL4, or Venticute. Of particular interest in these cases are the biomimetic methods that are utilized to capture the functional motif of wild type lung surfactant proteins (SP-B or SP-C). As stated earlier, even with the protein sequence identified, synthesis is quite challenging, therefore some researchers have used truncated or modified peptide versions as well as peptoid structures in their lung surfactant replacement strategies^{82,85}. Many of these methods have shown successful results and each contain specific advantages. Many available lung surfactant replacements both synthetic and extracted, show comparable behavior despite different compositions. This suggests that either the mixture may be unimportant or that the composition has yet to be optimized⁴.

Chapter 2. Research Objectives

Our research is focused on the effect the main oxidant component of photochemical smog, ozone, will have on the functioning of lung surfactant films. The novel experimental set-up we employ allows direct exposure of spread monolayers to controlled ozone concentrations and real time monitoring of the changes this may induce in the film pressure. We have used both model lipid and Survanta monolayers for these experiments which allows for the comparison of results with and without the surfactant proteins. Such model monolayers are commonly used to investigate the roles of lipids and proteins in film composition. Lipid mixtures as well as the single components have been analyzed and compared. Lung surfactant contains unsaturated lipids as a major component; these unsaturated lipids are susceptible to oxidation at the double bond within their alkyl chains. Cleavage of the alkyl chain will remove a significant portion of their hydrophobic character and may consequently change their surface activity and film cohesion. We are interested in how the oxidation reaction is changing the surface activity, morphology and especially the rheological properties of the lipid films and how these changes may affect normal respiration. These interfacial properties have been used by other groups to reveal the importance of film composition in achieving the needed mechanical behavior. Our experimental set-up is centered on a pendant drop instrument which allows the measurement of both surface activity as well as rheology, making this a versatile approach. The greatest advantage of the pendant drop set-up however, is the ability to easily control the reaction environment, allowing us to investigate how oxidative gas phase reactions change the film properties.

The thesis research will be presented in the form of three manuscripts (Chapters 3-5), each investigating specific perspectives of lung surfactant films. The first manuscript focuses on lipid structure and the relationship with dilational film rheology. The second manuscript describes the changes to surface properties ozone exposure induces in pure lipid films. The third and final manuscript consists of a comparison between ozone induced surface property changes to pure lipid films and Survanta, which contains the surfactant proteins SP-B and SP-C. Chapter 6 discusses the findings as a whole and also discusses oxidized lung surfactant with respect to normal respiratory physiology in terms of surface activity and rheology. The following is a description of the objectives of each manuscript and how they collectively describe the common theme of lung surfactant film behavior and rheology following ozone exposure.

2.1. Contributions of Authors

All research experiments and thesis manuscript drafts have been performed and written by Justin W. Conway under the supervision of Dr. Christine DeWolf. Dr. Rolf Schmidt also contributed to our research through discussions regarding data interpretation and experimental set-ups.

2.2. Lipid Structure and Rheology

Presently in the literature there exists very limited information on both lipid chain and head group structure influence with respect to lipid film rheology¹⁵. For this reason a systematic study varying lipid chain saturation and head group while measuring viscoelasticity was performed on a series of PC and PG lipids. The PC and PG lipids are our main focus as they are the two major components of natural lung surfactant²⁹. This is

therefore a logical starting point for the eventual interpretation of any future results involving the chemical modification or composition of lung surfactant films. The experiments in this publication were focused on the film organization and rheological differences between PC and PG lipids with comparable degrees of saturation. The PC lipids studied were DPPC, POPC, and DOPC. The PG lipids studied were DPPG, POPG, and DOPG. The comparison of viscosity and elasticity measurements between the PC and PG lipids will be used to determine the respective influence of head group and side chain structure on these parameters. The information from these experiments will emphasize the structure-organization dependence of viscoelasticity.

2.3. Model Lung Surfactant Films of POPG and POPG/DPPC (20:80)

Lipid monolayers of pure POPG and POPG/DPPC (20:80) mixtures have been used as model systems for the phospholipid film at the surface of the alveolar sacs. We exposed the monolayer to controlled concentrations of ozone and monitored the resulting changes to surface activity, morphology and rheology. It is well established that the lung surfactant lipid film must achieve both high surface tension reductions as well as rapid spreadability⁷⁻⁹. The influence of both surface tension and film fluidity can be further investigated using dilational rheological measurements of monolayer films. Dilational rheology is significant to lung surfactant films as it describes the viscosity and elasticity of the film during respiration. These experiments focused on surface activity and cohesive changes to POPG alone and in the POPG/DPPC (20:80) mixture following ozone induced oxidation. ESI-MS experiments have been used to determine if POPG is completely consumed during ozone exposure and to identify the oxidation reaction

products. Compression isotherms, dilational rheology and BAM have been used to determine the changes to surface behavior and film morphology induced by the oxidation reaction. These experiments provide information on the organizational changes in the monolayer generated by ozonolysis which may lead to altered film surface activity, rheology and morphology.

2.4. *Survanta Film Behavior*

The final manuscript included in the thesis is focused on the surface activity, morphology, and rheological changes following ozone exposure in Survanta. Survanta is a clinically used lung surfactant replacement which contains a mixture of phospholipids and membrane proteins. A comparison with our initial results of model POPG/DPPC mixture films yields information on the role the membrane proteins serve as well as their susceptibility to ozone induced oxidation. Furthermore, it is known that Survanta contains a mixture of PC and PG phospholipids therefore the rheological information from the pure lipid models will prove useful for data interpretation. Survanta films have been investigated using compression isotherms, BAM and pendant drop rheology techniques. Compression isotherms and recompression experiments on Survanta films before and after ozone exposure have been used to determine if the oxidation is reducing the surface activity of certain components. These experiments also provided information on how the mechanical roles of the surfactant proteins might be changing following ozonolysis. The rheology and film morphology changes induced by oxidation in Survanta films have also been measured. This information was compared to the pure and mixed lipid films in order to determine how surfactant protein interactions may influence the

film behavior. These results can then be used to make conclusions with respect to respiratory health and ozone inhalation.

Chapter 3. A Rheological Comparison of Molecular Structure Effects in a Series of Phosphoglycerol and Phosphocholine Lipids

3.1. Abstract

The rheological properties of a series of phosphocholine (PC) and phosphoglycerol (PG) lipid monolayers have been investigated to compare the influence of head group and side chain structure on viscosity and elasticity. The PC and PG lipids differ in terms of inter-lipid and lipid-subphase molecular interactions arising from head group chemical properties. Isotherms and dilational viscosity/elasticity measurements have been performed using the oscillating pendant drop method. The comparison of film viscosity measurements between the PC and PG lipids indicates that this parameter is dominated by head group interactions. The PG head groups show evidence of strong lipid-lipid and lipid-water interactions. The results of these experiments indicate significant similarities in the elasticity of LE unsaturated lipid films. The elasticity measurements appear to be dependent on lipid chain structure with PC films showing slightly higher elasticity. The information from these experiments emphasizes the structure-organization dependence of viscoelasticity.

3.2. Introduction

The dynamic rheological properties of lipid membranes are critical for understanding biological processes, pharmaceutical applications, health issues as well as

industrial processes (optical components, photography and food industries)⁸⁶. The rheological properties of a biological membrane are influenced in particular by the interactions of its constituent lipids¹⁵. These inter-lipid interactions generate a cohesive force in a monolayer which opposes film compression and expansion. The magnitude of these opposing forces is quantified in a rheological study using surface viscosity and elasticity. These two parameters can be used to describe membrane relaxation after the system is perturbed by an outside force. For example, when cell membranes encounter a stress such as protein insertion or osmotic pressure, they must respond and accommodate the packing strain or increased cell volume. Membranes adjust their shape and accommodate these stress/strain factors through intrinsic flow and deformation properties that are highly dependent on their lipid composition. This study will determine the rheological properties of several ubiquitous membrane lipids and how chain and head group structure influence membrane viscoelasticity.

The flow and deformation of a lipid film is described by viscosity and elasticity, respectively. Viscosity is a measure of the resistance of the molecules in a material to move with respect to their neighbors when subjected to an applied force. Elasticity is a measure of reversible/non-reversible geometric deformation and recovery of the material following an applied force and is often described by Hooke's law. Lipid membranes exhibit a combination of viscous and elastic behavior. Such materials are said to be viscoelastic and are classified as non-Newtonian fluids. The rheological behavior of these fluids under an applied force is commonly expressed using a Maxwell model, which describes viscoelasticity as a two component system connected in series¹⁴. In the Maxwell model, the viscosity component can be envisioned as a dash-pot responsible for

energy dissipation while the elasticity component can be likened to a spring accounting for energy storage.

Lipid and membrane protein monolayers at the air/water interface are frequently used as model systems to investigate membrane adsorption, surface activity and rheology. Although monolayers have been extensively studied in terms of membrane adsorption and surface activity there are comparatively few examples of dilational rheology studies on lipid films. Previous rheology studies on lipid monolayers have shown varied viscoelastic film behavior attributed to chain and head group structural differences. Furthermore, the majority of lipid rheological research to date has been focused on dipalmitoylphosphatidylcholine (DPPC) alone and in mixtures. This is due to the importance that DPPC has in lung surfactant films and cellular membrane composition in general.

Some of the first dilational rheology results are reported for DPPC monolayers^{69, 70,86}). These researchers linked changes in rheology to the phase behavior of the lipid films. Wüstneck *et al.*^{71-73,80} have shown that the viscoelasticity of these films is sensitive to both temperature and oscillation frequency. Vrânceanu *et al.*¹⁴ investigated DPPC, DOPC and their respective mixtures with cholesterol to determine how oscillation frequency and amplitude affect rheology. They found that saturated lipid films exhibit consistently higher viscosity and elasticity at all surface pressures compared to unsaturated lipids and that viscosity is much more dependent on dynamic conditions than elasticity. Work by Anton *et al.*¹⁵ is one of the few examples of research which examines lipid film rheology in terms of how both lipid side chains and head group structures influence measured viscoelasticity¹⁵. These experiments determined the rheology of a

series of phosphatidylcholines (PC) and phosphatidylethanolamines (PE) at a single equilibrium adsorption surface pressure. The side chains of PC and PE were kept the same in order to observe how head group interactions change the viscosity and elasticity. They found that inter-lipid and lipid-subphase head group interactions significantly influence the film rheology when comparing PC and PE lipids with the same chain structures.

Dilational rheology measurements can be performed using techniques such as oscillating barriers on a Langmuir trough and more recently using pendant drop/bubble set-ups. All of these set-ups are able to cyclically compress and expand a monolayer spread at an interface while measuring surface pressure. There are several advantages to using the pendant drop/bubble set-up. Viscoelasticity measured using a pendant drop apparatus homogeneously compresses and expands a monolayer during the oscillation sequence. Also, the surface pressure of the film is measured using a visual profile so there is no direct contact between the film and measuring device as in a Langmuir trough which uses a Wilhemy plate to measure surface pressure. Together, these advantages limit localized domain formations in a monolayer compressed with barriers (Langmuir trough) and remove any surface measurement errors that may be introduced by direct contact with a film.

The research presented here relates film rheology to lipid chain and head group structure over a range of surface pressures. Probing these structural interactions will lead to greater insight into the lipid interactions of biological systems such as lung surfactant or cellular membranes. Information pertaining to how the membrane composition influences the rheology of the system is useful for understanding any process occurring at

a lipid interface. The lipids we have chosen to investigate are PCs and phosphatidylglycerols (PGs) because of their ubiquity in animals and plants and relevance to lung surfactant films. PCs are the most prominent membrane lipids in all organisms, and PGs are an important component of plant⁴⁷ and bacterial membranes⁸⁷ as well as having a role in animal respiration⁴⁷. The lipid chain structures used in this study are dipalmitoyl (DP), palmitoyloleoyl (PO), and dioleoyl (DO), for both the PC and PG headgroups (see Figure).

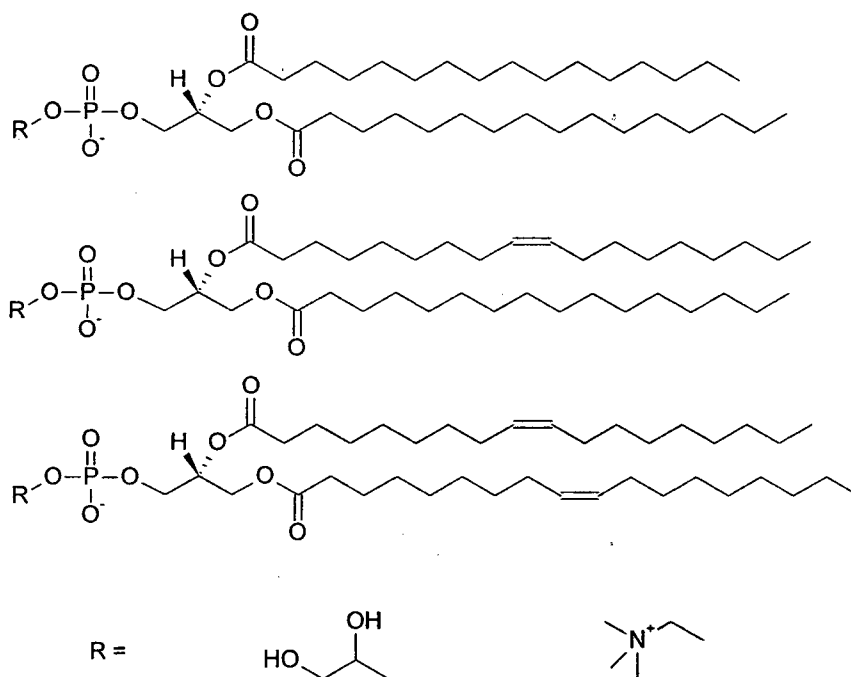


Figure 3.1. PC and PG lipid structures. From top to bottom; dipalmitoyl (DP), palmitoyloleoyl (PO), dioleoyl (DO).

3.3. Methodology

Dipalmitoylphosphotidylcholine (DPPC), 1-palmitoyl-2-oleoyl-phosphotidylcholine (POPC), dioleoylphosphotidylcholine (DOPC), dipalmitoylphosphatidylglycerol

(DPPG), 1-palmitoyl-2-oleoylphosphatidylglycerol (POPG), and dioleoylphosphatidylglycerol (DOPG) were used as received (Avanti Polar Lipids, Alabaster, AL, USA; purity > 99%). Ultrapure water (resistivity $18.2 \text{ M}\cdot\Omega \text{ cm}^{-1}$) is obtained using an Easypure II LF purification system (Barnstead, Dubuque, IA, USA). HPLC grade chloroform is used as received (Fisher Scientific, Pittsburgh, PA, USA) as the spreading solvent in all monolayer experiments.

All experiments were performed on a profile analysis tensiometer (PAT) (SINTERFACE Technologies, Berlin, Germany). This set-up employs axisymmetric drop shape analysis (ADSA) to relate the drop curvature obtained from a visual profile of a pendant drop to the interfacial pressure^{16,86}. ADSA specifically applies the Young-Laplace equation to determine the interfacial pressure¹⁶. Both isotherm compressions and rheological oscillation experiments were performed with this instrument.

Monolayers are spread using a lipid chloroform solution of 0.1 mM at the surface of a 10 to 15 μL (surface area of 25 - 35 mm^2) pendant drop of water formed at a capillary tip. Spreading volumes ranging from 0.4 to 0.9 μL were deposited on the drop surface, which is then left at rest for 3 minutes to allow the evaporation of the spreading solvent. Monolayer compression is achieved by decreasing the drop volume with an automated micro-syringe pump, thus reducing the available surface area. Prior to monolayer compression, the pendant drop volume is increased to 26 μL (40 mm^2), and left for 3 minutes to allow monolayer equilibration. Surface pressure-area isotherms are carried out using a molecular compression speed of $0.13 \text{ \AA}^2 \text{ molecule}^{-1} \text{ s}^{-1}$. The drop temperature for all compression experiments is room temperature (23 °C). It should be noted that isotherm compressions of certain lipids such as DPPC performed on a pendant

drop do not show the specific characteristics of phase transitions⁷¹ observed on a Langmuir film balance.

The monolayers used for rheological experiments are deposited and prepared in the same manner as above. The rheological measurements are then performed by compressing the lipid monolayer to a specific target pressure at a drop size of 10 μL (20 mm^2). The drop volume is then sinusoidally oscillated, generating an oscillation in the available surface area. The monolayer is repeatedly expanded and compressed which leads to changes in surface pressure. A complex elastic modulus can be calculated by relating the variation in surface area to the surface pressure response⁸⁶. Oscillations in drop surface area and consequent surface pressure response are analyzed using a Fourier transform to fit a surface pressure response curve. The dilational viscosity and elasticity are then determined using this fitted curve^{14,16}. Dilational rheology measurements are sensitive to the frequency and amplitude of oscillation^{14,78,80}. In particular, oscillation frequencies should not exceed values which disrupt the Laplacian shape of the pendant drop. This frequency range was experimentally determined to correspond to a range of 0.005-0.200 s^{-1} . In our set-up all experiments are performed with an oscillation frequency of 0.025 s^{-1} . Also, the amplitude of oscillation of the drop surface area should remain under 10% of the actual drop size^{14,88}. Our experiments are performed using amplitude oscillations of 2.5% of the drop size to prevent monolayer collapse and loss of the pendant drop.

3.4. Results and Discussion

The rheological behavior of lipid films has been previously interpreted relating the extent of cohesive forces within a monolayer to the lipid packing^{69,78,14}. The increased

lipid packing as a monolayer is compressed through gaseous (G), liquid expanded (LE), and condensed (C) phases increases lipid interactions. Therefore identification of the monolayer phase state can be correlated to the relative strength of cohesive forces within a film. It is these cohesive forces that produce the specific viscoelastic properties for individual lipid monolayers. The monolayer phase is determined by comparing the shape of compression isotherms for all PC and PG lipids. Within each respective PC and PG lipid group the phase behavior will be correlated to the viscoelasticity exhibited by each lipid film.

The lipid monolayers have been characterized using compression-isotherms performed on a pendant drop. In Figure 3.2, graphs on the left and right correspond to the PC and PG lipids, respectively. All isotherms are in good agreement with similar studies and indicate that saturated lipids reach the greatest surface pressures and lowest molecular areas^{56, 89-92}. DPPC and DPPG are the only lipids investigated which exhibit a condensed phase. All other lipids examined here contain at least a single unsaturated chain and remain in an LE phase until collapse.

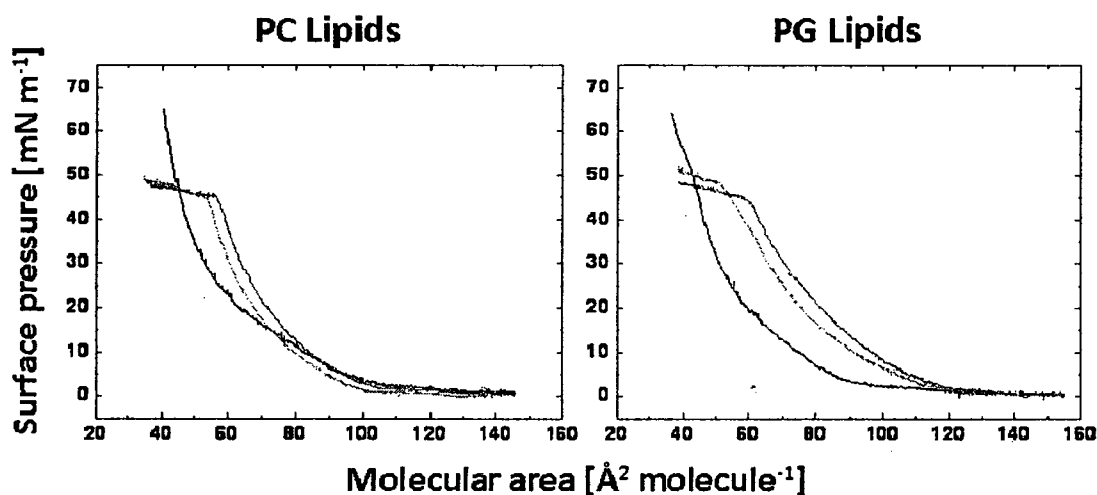


Figure 3.2. Isotherms of PC and PG lipid monolayers on water at 23 °C. DPPC/DPPG (—), POPC/POPG (---), DOPC/DOPG (-·-·-).

Figure (left) shows the rheological measurements performed on the PC lipids. The viscosity measurements of the PC lipids indicate that DPPC has the highest values reaching approximately 40 mN s m^{-1} . DPPC viscosity increases above that of the unsaturated lipids starting at pressures between $10\text{-}15 \text{ mN s m}^{-1}$, which is in the range that DPPC is known to enter a LE-C phase transition^{14,80}. This increase in viscosity due to a phase transition corresponds to increased chain-chain interactions. Vrânceanu *et al.*¹⁴ also noted similar behavior for DPPC, including the almost constant viscosity until the end of the LE-C transition. POPC and DOPC viscosities maximally reach 15 mN s m^{-1} over the same surface pressure range. Rheological measurements are limited to film pressures greater than 5 mN m^{-1} , since oscillations below this pressure do not generate measurable surface pressure changes⁹³.

The organization and orientation of densely packed lipid monolayers maximizes the extent of non-covalent interactions. In this close packed state the greatest viscosity and elasticity values are expected to be exhibited by saturated lipid films as is the case for DPPC^{69,71,78}. Previous work has also shown that viscosity is considerably more sensitive to frequency and harmonic distortions at high surface pressures¹⁴. Based on this information, data is not shown for films over 40 mN m⁻¹ where artifacts of oscillations within an over-compressed film and/or the presence of collapse material are possible. The rheological results for all PC lipids agree with the molecular packing interpretation. The introduction of unsaturated alkyl chains limits the extent of organized cohesive molecular interactions within a monolayer in this pressure range.

All PC monolayers measured below 25 mN m⁻¹ show low, near constant viscosity values indicating persistent film fluidity attributed to the presence of LE phase (Figure 3.2). These results are in good agreement with relaxation experiments on DPPC films by Wüstneck *et al.*⁷¹. This work has shown that below 25 mN m⁻¹ following a compressional or dilational stress, a DPPC film consistently regains a constant surface pressure within 10 minutes of the event. The fact that these DPPC films consistently rearrange to attain a constant surface pressure within similar time periods, indicates comparable film fluidity at all pressures below 25 mN m⁻¹ as seen in our DPPC measurements.

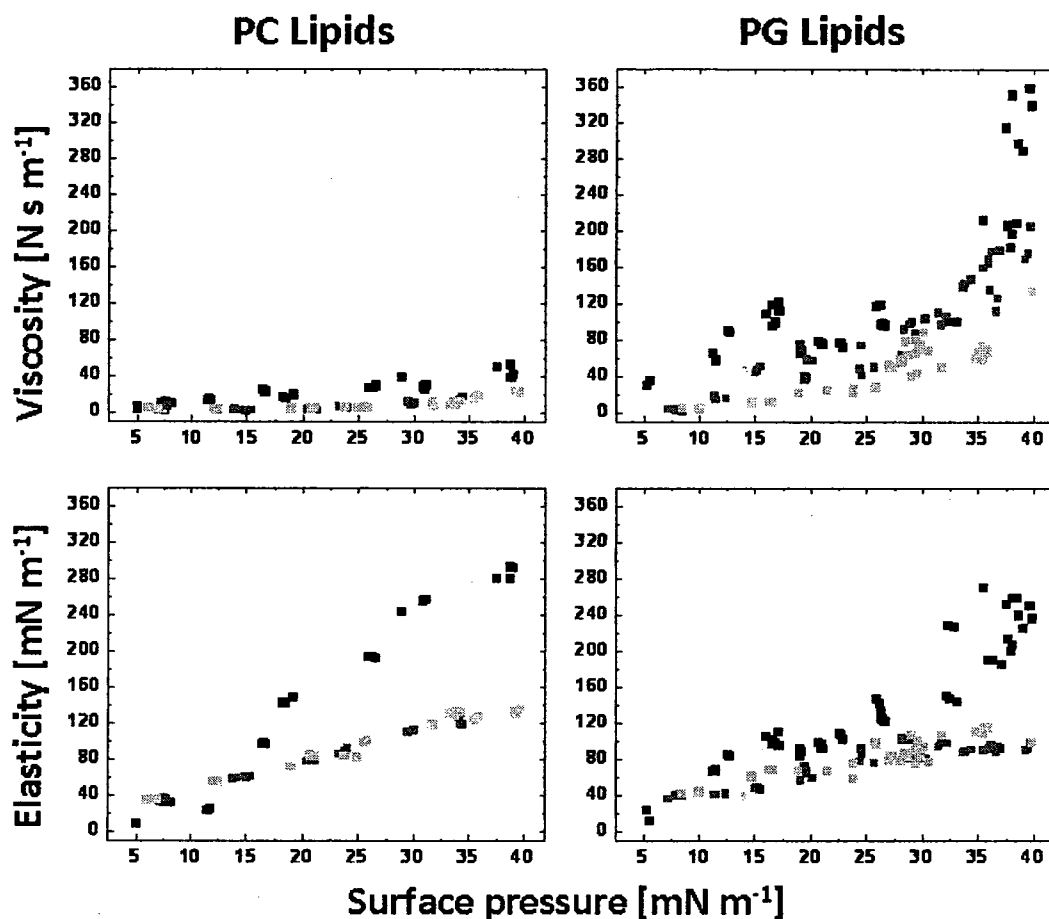


Figure 3.3. Dilational viscosity (top) and elasticity (bottom) of PC (left) and PG (right) lipid monolayers on water at 23 °C. DPPC/DPPG (■), POPC/POPG (◼) and DOPC/DOPG (⊙).

The elastic measurements in Figure (bottom) also underscore the relationship between molecular organization and film cohesion. The elasticity of DPPC as a function of pressure exhibits the greatest slope within the PC lipids measured. DPPC elasticity reaches a maximum value of approximately 290 mN m^{-1} at a surface pressure of 39 mN m^{-1} . Other groups working with a similar PC and phosphatidylethanolamine (PE) lipid series have also shown that the saturated lipids have both higher viscosity and elasticity than the corresponding unsaturated ones^{14,15}. POPC and DOPC have closely matching

values with a decreased slope relative to DPPC. The elasticity of POPC and DOPC films increases to a maximum value of approximately 145 mN m^{-1} at a surface pressure of approximately 40 mN m^{-1} . The greater slope in elasticity above 15 mN m^{-1} of DPPC monolayers may also be attributed to the presence of condensed phase following a LE-C phase transition. The comparable elasticity values for POPC and DOPC as surface pressure is increased, indicates that elasticity is related to monolayer phase and is independent of the number of unsaturated chains. Therefore, the similarities between POPC and DOPC viscosity and particularly elasticity are a consequence of their monolayers remaining in an LE phase until the collapse pressure. Vrânceanu *et al.* 2007¹⁴ have shown that films comprising lipids which do not show a LE-C transition such as POPC and DOPC have a smoother and more linear viscoelastic increase as also seen in our results.

Figure (right) shows the rheological measurements performed on the PG lipids. DPPG and DOPG respectively have the highest and lowest viscosity values as expected from their saturated and unsaturated structures. The asymmetrically substituted POPG lipid displays viscosity values intermediate to the fully saturated and fully unsaturated lipids. This is different than the observed unsaturated PC lipid trends. As can be seen from Figure, POPC and DOPC actually have overlapping values as surface pressure increases and lack the differentiation in viscosity seen in the PG lipids. A comparison of PG and PC viscosity at 17 mN m^{-1} is a good example of the relative extent of viscosity differentiation. At this pressure DPPG exhibits values nearing 115 mN s m^{-1} , POPG 50 mN s m^{-1} , and DOPG 16 mN s m^{-1} . At a similar surface pressure, the PC lipids (Figure) all exhibit elasticity values ranging from 5 to 25 mN s m^{-1} . This indicates that the

presence of the glycerol head group favors stronger intermolecular interactions leading to higher viscosities.

DPPG viscosity exhibits a roughly linear initial increase to 17 mN m^{-1} , at which point the viscosity appears to remain constant between 20 and 25 mN m^{-1} . Viscoelastic plateau regions such as this have previously been observed^{69,78} for lipids known to exhibit LE-C phase transitions. During this transition, a rise in viscosity is not observed, due to the decreasing surface area simply shifting the relative proportions of LE and condensed phase domains^{69,78}. However, Langmuir trough and BAM experiments by Hidalgo *et al.*⁹⁴ have demonstrated that DPPG exhibits a direct G-C phase transition. Furthermore, no LE-C phase transition was ever observed for DPPG on pure water at room temperature in our pendant drop experiments.

The isotherms show an inflection point at 20 mN m^{-1} , which is approximately at the beginning of the constant viscosity region (Figure 3.2). This inflection point indicates the occurrence of a molecular rearrangement. Previous grazing incident x-ray diffraction (GIXD) work has shown a tilting transition to a hexagonal packing of upright oriented molecules for DPPG on pure water between 35 mN m^{-1} and 40 mN m^{-1} ⁹⁵. It may be that these transitions occur at lower pressures for isotherms performed on a pendant drop. Several groups have also noted pendant drop isotherm behavior deviating from Langmuir trough experiments due to parameters such as spreading conditions or compression speeds⁸⁹. The attribution of the inflection point in the DPPG isotherm (Figure 3.2) to a tilt angle transition is supported by the significant changes in the slope of viscosity with increasing pressure, which have been known to coincide with phase transitions¹⁴. POPG

and DOPG do not exhibit any distinct plateau region in viscosity as they exhibit a LE phase until collapse.

The elasticity measurements of the PG lipids in Figure also exhibit distinct differences for saturated and unsaturated lipids. However where viscosity measurements of each of the respective PG lipids shows a distinct trend, the elasticity of lipids which contain at least one unsaturated alkyl chain are quite similar. DPPG has the highest values ranging from 0 to 265 mN m^{-1} , followed by POPG and DOPG which both display elastic values ranging from 0 to approximately 100 mN m^{-1} . The high elasticity seen in saturated PG lipids is consistent with our observations for the PC lipids and a similar series of PEs and PCs^{15,14}. As observed for the PC unsaturated lipids, POPG and DOPG appear to have comparable elasticity values attributed to the persistence of an LE phase due to unsaturation which yields similar monolayer organization. This observation suggests that elasticity is much more dependent on film phase behavior and chain interactions than viscosity. Anton *et al.*¹⁵ working with similar PC and PE lipid structures also show results indicating that elasticity is strongly affected by chain saturation but viscosity does not significantly change. The PG unsaturated lipids also exhibit a greater scatter of elastic measurements relative to the corresponding PC lipids. This may be attributed to the stronger intermolecular interactions, namely hydrogen bonding occurring between the glycerol head groups^{96,97}.

The rheological measurements in Figure are in good agreement with other publications for studies of similar systems^{14,71-73,88} however, the experimental set-up for measuring dilational rheology will influence the results obtained. For example, the range of viscoelastic values obtained for DPPC monolayers differs for Langmuir film balance

oscillating barrier experiments^{69,78}, pendant drop stepwise compression-dilations⁹³ and captive bubble methods¹⁵. However, independent of the measuring tool, the interpretations will remain valid with respect to our experimental observations. The viscoelastic values measured for the PG and PC lipids demonstrate that monolayer cohesive properties are directly related to the molecular organization based on chain structure and head group interactions.

The PG and PC lipids show viscosities which differ significantly. PG lipids have greater viscosities at all surface pressures compared to the PC lipids and show a greater initial increase in this parameter as pressure increases. The largest differences in viscosity between the PG and PC lipids are observed at higher surface pressures. In this high pressure region DPPC monolayers exhibit the highest viscosity of all the PC lipids. However, the values of DPPC are relatively low compared to DOPG films measured over the same pressure region. This comparison indicates that even the most saturated PC lipid (DPPC) does not reach the viscosity of the most unsaturated PG lipid (DOPG). This observation implies that although lipid chain structure plays an important role in monolayer organization, the head group structure strongly influences the measured viscosity. For example, stronger PG head group interactions, likely hydrogen bonding, result in a significant difference between POPG and DOPG LE phase viscosity. This difference in viscosity is not observed for POPC and DOPC LE phases. Previous work has shown that lipids with hydrogen bonding potential exhibit strong inter-lipid and lipid-water interactions that influence surface behavior^{15,89,98,99}.

The saturated lipids in both the PG and PC groups show the highest elasticity relative to their respective unsaturated lipids. A comparison of PG and PC elasticity

indicates that PC lipids consistently exhibit slightly greater film elasticity. For a given head group, the unsaturated lipids have comparable elastic properties which corresponds to elasticity being highly dependent on the phase of the monolayer rather than the number of unsaturated chains. The elasticity of all lipids with the exception of DPPG appears to reach a maximum at high surface pressure measurements. In the case of the PC lipids the elasticity actually begins to decrease following this maximum point, an event which has been previously observed for DPPG films⁷¹. Wüstneck *et al.*⁷¹ postulated that at high surface pressures there is a strong mechanical resistance towards further monolayer oscillations. This resistance to further oscillations occurs as lipids maximize chain-chain interactions through orientational and organizational adjustments as surface area becomes limited. This would explain the decrease or limited film elasticity observed at higher surface pressures in our experiments.

The structure of the chains in the PG and PC lipids are the same therefore the rheological differences must be related to the head groups. A significant distinction between PG and PC lipids is that PGs contain an overall negative charge while PCs are zwitterionic. The electrostatic repulsion between PG head groups leads to an effectively larger head group volume. This may cause weaker inter-lipid hydrogen bonding¹⁰⁰ and induce chain tilting⁹⁷. The phosphate and glycerol portions of the PG head group have been shown to participate in inter and intra molecular hydrogen bonds⁹⁸⁻¹⁰¹. It has been suggested that intramolecular hydrogen bonding between the glycerol moiety and the phosphate may shield some of the effective electrostatic repulsion through a hydration-like interaction¹⁰¹. The charge repulsion may be further reduced by the intercalation of water molecules at the negatively charged phosphate in the head group. This interaction

has been observed using FTIR studies looking at shifts in frequency from hydrogen bonding. Pimthon *et al.*¹⁰⁰ have also shown that the first hydration shell of the glycerol hydroxyls contains on average 3.05 and 3.29 water molecules which may partially shield some of the PG charge. However, the degree of DPPG head group hydration decreases with decreasing molecular area⁹⁷. Therefore intramolecular hydrogen bonds become increasingly important towards electrostatic shielding in the head groups.

Previous work⁹⁹ comparing lipid head groups which may or may not hydrogen bond to a water subphase has shown differences in their interfacial orientation. It was shown that hydrogen bonding between lipid head groups and water causes lipids to effectively penetrate deeper into a water subphase. PG lipids have previously been shown to participate in hydrogen bonding with a water subphase^{89,98,99}. The rheological result of lipid-subphase hydrogen bonding was investigated by Anton *et al.*¹⁵ using monolayers of DPPC and DPPE. DPPE possesses a head group which participates in hydrogen bonding with a water subphase much more effectively compared to DPPC. X-ray reflectivity results show that DPPE actually sits 1-2 Å deeper in the subphase than DPPC⁹⁹. Anton *et al.* concluded that the deeper penetration of the DPPE head groups into the water subphase generates a more hydrated state which will influence the monolayer viscoelasticity. The result of greater subphase penetration is an anchoring effect which impedes the interfacial lipid displacement of PG molecules at the surface thereby increasing film viscosity. PG lipids therefore experience a frictional drag as the lipids flow across the water subphase during the oscillation experiments¹⁵. Our experiments show that the PGs consistently exhibit a significantly greater viscosity than the PCs which likely do not sit as deeply in the subphase.

A second consequence of the PG head group water penetration is that in this position the lipid side chains have a reduced amount of non-hydrated chain length with which to interact and generate film cohesiveness¹⁵. Since elasticity has been shown to be dependent on lipid chain interactions, lipids which hydrogen bond and penetrate more deeply into the water subphase will have reduced elasticity. Our experiments show that PGs consistently exhibit a lower elasticity than the PC lipids since PC lipids are not as hydrated and will have more alkyl chain interactions. This was also observed by Anton *et al.* who measured higher elasticity for PC lipids compared to PE lipids with the same side chain structures¹⁵.

Hydrogen bonding may also occur between PG head groups which contributes to greater inter-lipid cohesive interactions. An example of this can be seen in work by Hidalgo *et al.*⁹⁴ who observed condensed phase formation of DPPG at zero surface pressures using BAM. The early condensed phase formation can be attributed to inter-lipid hydrogen bonding and is not seen in DPPC monolayers. The earlier condensed phase material may be linked to the greater slope of viscosity as a function of pressure compared to the PC lipids noted in our experiments. We propose that PG lipid monolayer rheology is affected by both lipid-subphase and lipid-lipid hydrogen bonding which generates greater subphase penetration and early condensed domain formation, respectively.

3.5. Conclusion

We have reported a systematic comparison of lipids with different head group and side chain substitution over a wide range of surface pressures. These results have shown that lipid head group and side chain structures have different effects on film rheology.

Viscosity is primarily determined by head group and subphase interactions. Stronger intermolecular interactions lead to significantly greater viscosity as exemplified by the PG films. Furthermore, distinctions in film viscosity between lipids with different chain structures require strong head group interactions. Elasticity is a measure of film cohesiveness, which was for the most part determined by chain interactions. Elasticity is therefore directly related to the monolayer phase state. Condensed and LE phase films can be expected to show distinct elasticity trends as observed in our experiments. For both the PC and PG lipids investigated, the introduction of unsaturated chains yields an LE film with similar elasticity. As PC and PG lipids are known to be the major components of lung surfactant in humans, a greater understanding of the rheological properties of each component may be used to help generate optimal lung surfactant replacement treatments.

Chapter 4. Surface Activity and Rheological Changes in Model Lung Surfactant Films Resulting from Ozone Exposure

4.1. Abstract

Lung surfactant comprises saturated and unsaturated lipid components in addition to the surfactant proteins. This lipid composition is required to achieve high surface pressure reduction while maintaining film fluidity. We have utilized model lung surfactant films (monolayers comprising 20% 1-palmitoyl-2-oleoyl-*sn*-glycero-3-phospho-1-glycerol and 80% 1,2-dipalmitoyl-*sn*-glycero-3-phosphocholine) to determine the effects on the unsaturated phospholipid component of exposure to an environmental oxidant, namely ozone. Changes in surface activity and dilational rheology have been examined using a pendant drop tensiometer while morphological changes have been examined using Brewster Angle microscopy. We have found that these lipids retain much of their original surface activity after oxidation. However, significant changes in surface rheology after exposure to ozone have been observed, in particular a decrease in monolayer viscoelastic properties. This may result in reduced physiological performance of the respiratory system.

4.2. Introduction

As respiration takes place, oxygen fills the lungs and crosses through a lipid membrane at the air-water interface^{2,3} located at the surface of the alveolar sacs. These

sacs resemble small air bubbles covered with a thin film of phospholipids and membrane proteins. This lipid film, termed lung surfactant, serves to reduce the surface tension acting to collapse the alveoli and, due to its composition, is able to rapidly compress and expand over the surface of the alveoli during respiration⁸. Therefore, the mechanical properties of the lung surfactant films are important for normal respiration. It is generally accepted that lung surfactant is a dynamic system in which lipids and membrane proteins work in conjunction to provide breathing function¹⁰².

Research into lung surfactant systems has investigated how the many surface active components work in coordination^{42,44,46}. One direct application of this research is to develop lung surfactant replacement therapies for an array of respiratory diseases and environmentally induced ailments, the most common examples being infant respiratory distress syndrome (RDS) and inhalation of atmospheric oxidants, respectively. Successful clinical treatments include synthetic pulmonary replacements containing biomimetic peptides⁸², purified lipids, and natural surfactant extracts from bovine lung lavages²⁹.

Lung surfactant films have been extensively investigated in terms of their phase transitions^{72,74}, surface morphology^{43,103}, synthesis, secretion, uptake¹⁰⁴, composition effects and temperature dependence⁷⁷. Mechanical properties as a function of lipid-lipid or lipid-protein interactions have also been studied^{78,80}. Much of the pioneering work revolved around the characterization of the lung surfactant behavior as well as the clinical applications towards treatment of respiratory diseases^{5,105}.

Environmental health hazards such as ozone in photochemical smog can cause serious respiratory complications^{22,24}. Inhalation of ozone has been shown to cause airway inflammation, coughing, shortness of breath, or even increased susceptibility to

bacterial infection^{36,39}. These biological responses are the result of both ozone pulmonary damage and the transmission of ozone toxicity through the lung surfactant membrane deeper into the extra-pulmonary tissues²⁰. Due to the high reactivity of ozone, the primary oxidation reaction will occur within the lipid lining of the lung airways; therefore ozone itself does not penetrate deeply into other tissues, a situation termed reactive adsorption³². The main products as ozone is inhaled are lipid ozonation products (LOPs) in the form of aldehydes, hydroxyl hydroperoxides, and Criegee ozonides created during the ozonolysis of unsaturated lipids. These secondary reaction products penetrate into deeper regions of the respiratory tract triggering an inflammatory response. Transmittance of ozone toxicity via the cascade of LOPs acting as secondary messengers has been proposed by several groups^{12,13,20}.

The effects of tobacco smoke oxidation^{18,19} and ozone exposure^{11,35} on model membranes have been examined and shown changes in membrane morphology, minimum surface tension and respreading. To our knowledge, the effects of environmental photochemical oxidants on the viscoelastic properties of lung surfactant have yet to be investigated. In this paper we describe the effects exposure to an airborne oxidant and production of LOPs, will have on the surface activity and dilational rheological properties of model lung surfactant films. The dilational rheology measurements yield quantitative information regarding the viscoelastic properties of the surfactant film which can be correlated to the recovery and spreadability of the phospholipid film as respiration occurs.

A mixture of saturated and unsaturated lipids provides the surface behavior necessary to fulfill the biophysical role of pulmonary surfactant. The lung surfactant film

composition must generate a large reduction in surface tension, about 70 mN m^{-1} to prevent alveolar collapse⁸, as well as allow rapid film compression and expansion as alveoli inflate and deflate. The lung surfactant film is comprised of 90% lipid component and 10% membrane proteins by mass²⁹. The latter comprises four lung surfactant membrane proteins with various roles in lipid compression/expansion dynamics, replenishment of the phospholipid film and prevention of bacterial infections^{3,51}. The lung surfactant comprises up to 80% saturated phosphatidylcholine (PC), predominantly dipalmitoylphosphatidylcholine (DPPC), and 10% unsaturated phosphatidylglycerol (PG) mainly 1-palmitoyl-2-oleoyl-phosphatidylglycerol (POPG)^{3,8}. The remaining 10% corresponds to minor lipid components such as phosphatidic acid, phosphatidylinositol, phosphatidylethanolamine and cholesterol. The saturated lipid components are required for large reductions in surface tension which minimize respiratory work while the unsaturated components are associated with facilitating the rapid compression and expansion of lung surfactant films over the alveolar surface^{3,8}. Since DPPC and POPG represent the major saturated and unsaturated lung surfactant components, mixtures of DPPC and POPG have been used at the air-water interface as simplified model monolayers for lung surfactant^{42,43,46}. We expose mixed monolayers of 20% POPG and 80% DPPC to controlled concentrations of ozone and monitor the resulting rheological changes.

4.3. Methodology

Dipalmitoylphosphatidylcholine (DPPC) and 1-palmitoyl-2-oleoyl-phosphatidylglycerol (POPG) were used as received (Avanti Polar Lipids, Alabaster, AL, USA; purity > 99%). Ultrapure water (resistivity $18.2 \text{ M}\Omega \text{ cm}^{-1}$) was obtained using an

Easypure II LF purification system (Barnstead, Dubuque, IA, USA). HPLC grade chloroform was used as received, (Fisher Scientific, Pittsburgh, PA, USA) for the spreading solvent in all experiments.

Lipid monolayers were spread from a 0.1 mM lipid solution in chloroform at the surface of a 10 μL (25 mm^2) pendant drop of water. After spreading volumes ranging from 0.4 to 0.9 μL on the drop surface, the drop is then left at rest for 3 minutes to allow the evaporation of the spreading solvent. Following this step, the pendant drop is expanded to 26 μL (40 mm^2), and again left for 3 minutes to allow lipid equilibration at the surface. Surface pressure-area isotherms are performed using a molecular compression speed of 0.13 $\text{\AA}^2 \text{ molecule}^{-1} \text{ s}^{-1}$. The initial drop surface area and temperature for all compression experiments was 40 mm^2 and 25 $^\circ\text{C}$, respectively.

With the exception of Brewster angle microscopy imaging, all experiments were performed on a profile analysis tensiometer (PAT) (SINTERFACE Technologies, Berlin, Germany). Axisymmetric drop shape analysis (ADSA) is used to relate the drop curvature obtained from the visual profile to the interfacial pressure^{16,86}. For rheological measurements, the lipid monolayer is initially compressed to a target pressure at a constant drop size of 10 μL (20 mm^2), after which the drop area is oscillated. Mathematically, a complex elastic modulus is derived relating the oscillation in surface area to the surface tension response⁸⁶. This complex elastic modulus is then separated into two components, the dilational surface elasticity and viscosity of the lipid monolayer. The frequency and amplitude of oscillation are known to be important parameters for dilational rheology measurements^{14,78,80}. The frequency of oscillation must be slow enough for the pendant drop to maintain its Laplacian shape, corresponding to a

frequency range of 0.005-0.200 s⁻¹. All experiments are performed with an oscillation frequency of 0.025 s⁻¹. In addition, the amplitude of oscillation should remain under 10% of the actual drop size, which corresponds to a maximum area change of 4 mm² (1 μL volume change)¹⁴. Rheological experiments performed at surface pressures below 30 mN m⁻¹ use amplitude oscillations of 7.5% of the drop size. At surface pressures above 30 mN m⁻¹, small changes in drop size result in large changes in the surface pressure, therefore a lower amplitude change of 2.5% is used to prevent drop detachment.

Ozonolysis of the lipid monolayer at the surface of a pendant drop is performed by isolating the drop in a reaction chamber with a volume of 40 mL. The reaction chamber is then flooded with controlled ozone concentrations using a digital mass flow controller (Aalborg, Orangeburg, NY) at a flow rate of 100 mL min⁻¹. An ozone generator (UVP, Upland, CA) is used as the ozone source and the concentration is monitored using an ozone monitor (2B Technology, Boulder, CO). Monolayers are exposed to 8 ppm ozone for 10 minutes, after which no further change in surface pressure was observed. Although a concentration of 8 ppm ozone is relatively high compared to environmental conditions¹⁰⁶, it is utilized as a proof-of-principle to demonstrate the effects of ozone exposure.

Lipid monolayers were imaged using Brewster angle microscopy (BAM) performed with an I-Elli2000 imaging ellipsometer (Nanofilm Technologies GmbH, Göttingen, Germany) The ellipsometer is equipped with a 50 mW Nd:YAG laser ($\lambda = 532$ nm). The BAM images were taken using a 20X magnification lens with a lateral resolution of 1 μm at an incident angle of 53.15°. All BAM experiments were performed on a Langmuir film balance (NIMA Technology Ltd., Coventry, U.K.) with a

compression speed of $0.09 \text{ \AA}^2 \text{ molecule}^{-1} \text{ s}^{-1}$ and at $25 \text{ }^\circ\text{C}$. Monolayers were prepared on a trough in the same way as on the pendant drop. Spreading volumes ranging $4\text{-}9 \text{ }\mu\text{L}$ were spread from a 1 mM chloroform solution. Monolayers were oxidized on the trough surface by enclosing the entire set-up to prevent instrument oxidation damage and then flooding the chamber with ozone. Monolayers were exposed to an ozone concentration of 8 ppm at a flow rate of 100 mL min^{-1} for 30 minutes.

An electrospray ionization mass spectrometer (ESI-MS) (Waters Micromass, Milford, MA) operating in negative mode with a sample flow rate of $1 \text{ }\mu\text{L min}^{-1}$ was used to identify the ozonolysis products. Samples were prepared by first spreading a monolayer film at the surface of a pendant drop and then exposing it to constant ozone concentration of 8 ppm for 10 minutes. An average of 5 drops was collected to ensure sufficient material for analysis (approximately 25 ng). The oxidized lipid material was dried under nitrogen and re-solubilized in a $2\text{:}1$ chloroform/methanol solution which was directly injected into the ESI-MS.

4.4. Results and Discussion

A mixture of 20% POPG and 80% DPPC (referred to as LS mixture for this manuscript chapter) is used as a simplified model system to represent lung surfactant. Figure 1 shows the isotherms obtained for this model lung surfactant mixture as well as the individual constituent lipid components. The isotherm of DPPC exhibits a condensed phase at lower molecular areas. The isotherm shape of POPG indicates that it remains in a liquid expanded (LE) state until the collapse pressure as expected for a lipid containing unsaturated alkyl chains under these conditions. It should be noted that the pendant drop isotherms in general exhibit similar properties as more conventional Langmuir film

balance isotherms but do display some differences. In particular, Li *et al.*⁸⁹ have shown that the isotherm of DPPC obtained on a drop does not contain the distinct phase transition plateau normally observed on a Langmuir film balance.

The LS mixture exhibits an isotherm with characteristics of both DPPC and POPG components. The shape of our LS mixture isotherms are in good agreement with similar studies using approximately the same mixture of DPPC and POPG⁴³ As seen in Figure up to surface pressures of 10 mN m^{-1} the LS mixture isotherm resembles that of DPPC. However, above 13 mN m^{-1} the isotherms begin to diverge, with the LS mixture exhibiting a much greater amount of film expansion due to the presence of the unsaturated lipid component which remains in a liquid expanded state. The isotherm slope of the LS mixture at high pressures indicates that the LS mixture comprises predominantly a condensed phase. The divergence of these isotherms begins at a surface pressure higher than that associated with a pure DPPC monolayer liquid expanded to condensed phase transition⁸⁹ suggesting a DPPC-rich condensed phase. At a surface pressure of approximately 45 mN m^{-1} the LS mixture isotherm displays a distinct kink, which corresponds to the collapse pressure of pure POPG. The kink observed in the LS mixture isotherm is therefore attributed to the expulsion of the liquid expanded phase rich in POPG into the subphase which is consistent previous research^{46,103}. Beyond this point, compression leads to a further increase in surface pressure attributed to the presence of a condensed phase, which does not collapse until much higher pressures between $60\text{-}70 \text{ mN m}^{-1}$. The LS mixture monolayer has a lower final collapse pressure than DPPC, further indication that this condensed phase is a DPPC-rich phase which contains some POPG molecules, limiting the molecular packing at high surface pressures. The

incorporation of some POPG into the DPPC matrix has previously been shown by grazing incidence X-ray diffraction^{43,107}.

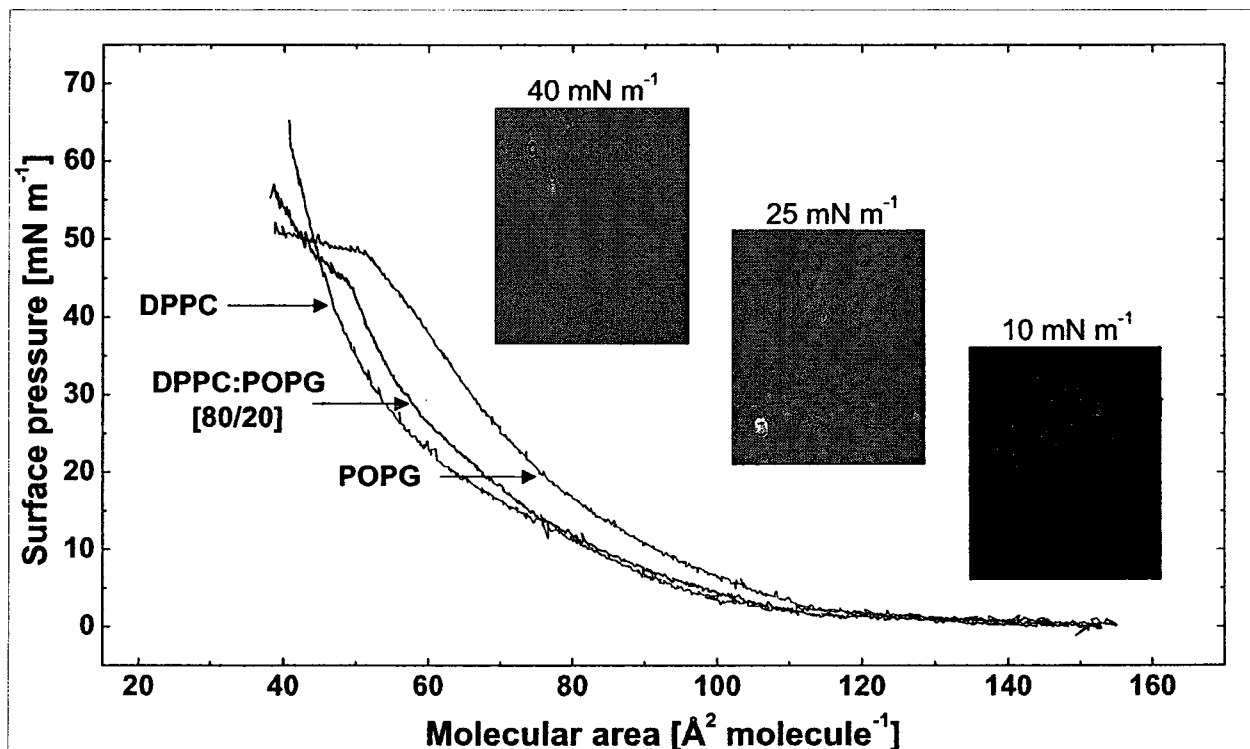


Figure 4.1. Isotherms of POPG, DPPC and POPG/DPPC (20/80) monolayers on water at 23 °C.

Inset: BAM images for the POPG/DPPC (20/80) monolayer at the surface pressures indicated.

Confirmation of phase separation into a DPPC-rich condensed phase and POPG-rich liquid expanded phase is obtained using BAM (Figure). In these images the dark regions correspond to the liquid expanded phase and the bright regions correspond to condensed phase lipid domains. Phase separation of DPPC and POPG is seen as early as 10 mN m^{-1} through the formation of small bright domains. At surface pressures nearing 40 mN m^{-1} a homogeneous film of condensed phase is observed with little collapse material confirming the expulsion of the unsaturated POPG from the interface. By contrast, in the presence of lung surfactant proteins some liquid-expanded phase material

is retained -at the surface while the remainder is expelled into membrane associated resevoirs necessary for efficient film respreading^{4,45,46}.

Lipid ozonolysis induces chemical modifications and consequent lipid re-organization. Ozone is known to react with carbon-carbon double bonds via the Criegee mechanism^{34,35,108}. In our model system the ozone-sensitive component is POPG, which contains a single unit of unsaturation in its oleoyl chain. Therefore, the major products of the ozonolysis, assuming a Criegee mechanism, are lipids with one intact palmitoyl chain and a cleaved 9 carbon alkyl chain functionalized with either an aldehyde, hydroxyl hydroperoxide, or a carboxylic acid group (Figure)^{30,109}. The reaction also generates nonanal and nonanoic acid¹¹⁰ which are soluble in the bulk phase (data not shown).

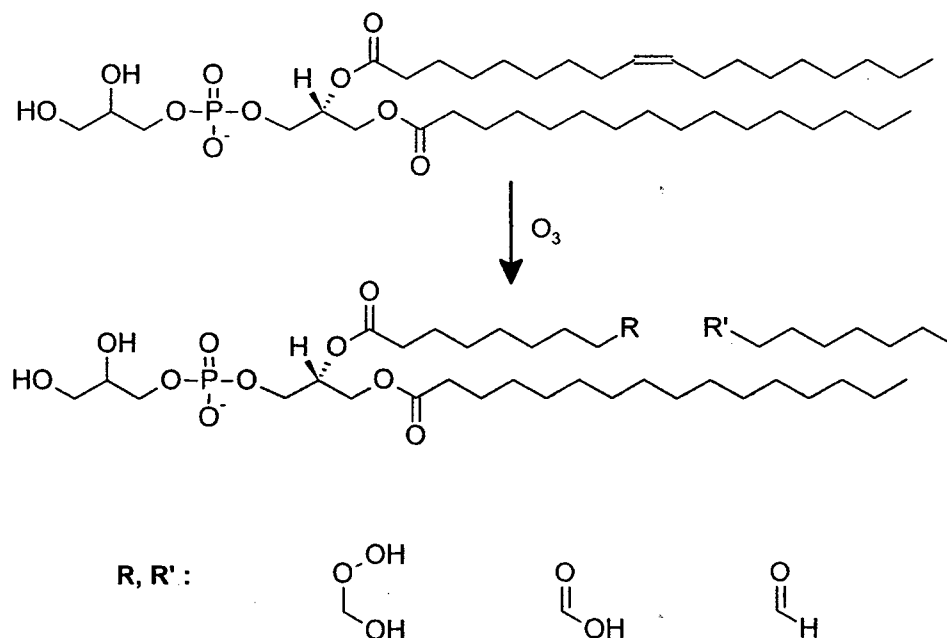


Figure 4.2. Reaction products for the surface ozonolysis of POPG monolayers assuming cleavage occurs via a Criegee mechanism.

The initial ozonolysis of POPG generates the aldehyde, 1-palmitoyl-2-(9-oxononanoyl)phosphatidylglycerol, the hydroxyl hydroperoxide, 1-palmitoyl-2-(9-hydroxy-9-hydroperoxynananoyl)phosphatidylglycerol and the carboxylic acid, 1-palmitoyl-2-(9-carboxynananoyl) phosphatidylglycerol³⁰ (see Figure). ESI-MS experiments have confirmed the presence of all three compounds (aldehyde, hydroxy hydroperoxide, and carboxylic acid) following the surface ozonolysis reaction of POPG monolayers and the complete loss of the POPG m/z peak (Appendix II).

Figure shows the changes in the isotherms for monolayers containing unsaturated phospholipids due to exposure to ozone. DPPC is unaffected by exposure to ozone¹¹⁰. On the other hand, the isotherms for films containing POPG show distinct changes following ozone exposure. Despite cleavage of one chain, the oxidized lipids do retain sufficient hydrophobic character to maintain high surface activity and yield isotherms characteristic of relatively insoluble monolayers.

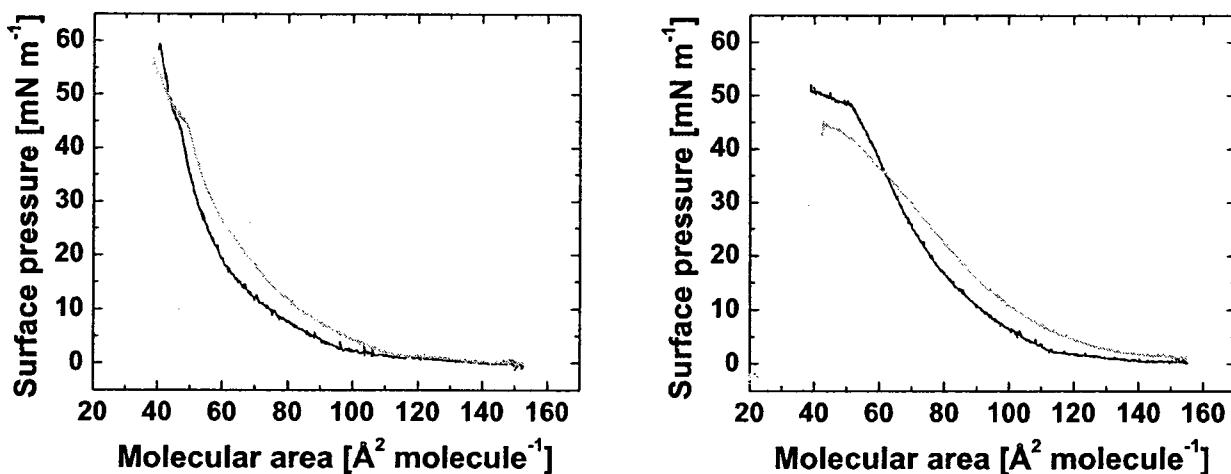


Figure 4.3. Isotherms of POPG (left) and POPG/DPPC (20/80) (right) monolayers on water at 23 °C before (—) and after (---) exposure to ozone.

Following the oxidation reaction, the isotherms of POPG show a clear reduction (approximately 5 mN m^{-1}) in the collapse pressure. The lung surfactant films serve to reduce the work associated with respiration via a reduction in surface tension. The maximum reduction in surface tension can be achieved by unoxidized lung surfactant films which attain surface pressures nearing 70 mN m^{-1} . Any reduction in maximum attainable surface pressure adds stress to the respiratory system. The oxidized LS mixture isotherm exhibits only a slight decrease, if any, in collapse pressure, attributed to the fact that the monolayer is predominantly non-reactive DPPC. At surface pressures above 40 mN m^{-1} , LS mixture films display a distinct kink in the oxidized monolayer isotherm. This kink is again attributed to the expulsion of reacted POPG into the bulk subphase.

The oxidized monolayer systems also exhibit isotherms clearly shifted to larger molecular areas with an altered slope indicating a higher compressibility. The film expansion in both systems (POPG and LS mixture) appears to be similar up until 30 mN m^{-1} despite only 20% reactive unsaturated component within the LS mixture. The expansion may be attributed to the modified surface properties of the cleaved lipid, in which the chains are not expected to pack as efficiently due to the addition of the polar moiety. Namely, it has been suggested that the polar ozonation products within the monolayer disrupt the lipid packing and facilitate the penetration of water molecules³⁵. Alternatively, even the soluble reaction products may remain at the water surface, *i.e.* favorable chain intermolecular interactions may overcome the expected drive of the nonanal/nonanoic acid fragments to enter the bulk phase. The presence of these molecules at the surface could cause the observed shift in the isotherm by reducing the available molecular area. The kinetic stabilization of partially soluble reaction products at

the air-water surface has previously been reported for mixtures of phosphatidylcholine and lysophosphatidylcholine (the product of PLA₂ enzymatic cleavage of the phospholipid)¹¹¹.

Lipid solubility in the water subphase before and after oxidation was examined by performing recompression experiments on monolayer films (data not shown). In these experiments, a monolayer was spread on the surface of a pendant drop and then subjected to 5 compression-expansion cycles. Subsequent compression cycle produces a shift to smaller molecular areas. This indicates that as the monolayer is compressed and expanded some of the lipids dissolve into the bulk phase and the ensuing re-adsorption is slow^{45,56}. Reproducibility of the extent of isotherm shifts was highly dependent on initial spreading conditions and the minimum area to which isotherms were compressed. However, in all cases the greatest loss of POPG monolayer material occurs between the first three recompression cycles where a steady shift in the isotherms is observed. Similar experiments have also found the greatest loss of material to the bulk phase occurs between the first compression cycles^{4,19}. Subsequent recompressions cycles exhibit a negligible loss of monolayer material indicating a solubility limit for POPG in the bulk phase. The reacted POPG monolayer displays a greater loss of surface material to the bulk phase when subjected to the same recompression conditions. Furthermore the reacted monolayer only reaches a solubility limit in bulk phase after four or more recompression cycles. This greater loss of monolayer material following exposure to ozone is attributed to the greater hydrophilicity of the reaction products. The LS mixture does not demonstrate a noticeable shift to reduced molecular areas during isotherm cycling, attributed to the high proportion of insoluble, saturated lipids which may mask

the loss of a similar proportion of POPG (oxidized or unoxidized). Alternatively, the interactions between the saturated and unsaturated components might reduce the loss of material to the subphase.

The intermolecular lipid interactions within a monolayer are directly related to the viscoelastic behavior, as they reflect the monolayers resistance to flow and strain during surface area oscillations^{78,112}. The viscoelastic parameters vary depending on the monolayer structural changes, organization and packing. In general, both viscosity and elasticity are known to increase as the molecular area decreases and lipids are packed closer together^{14,72}. Fully saturated alkyl chains are able to maximize their chain-chain interactions through efficient molecular packing as the available surface area is reduced. The introduction of unsaturated units within the alkyl chains significantly reduces the packing efficiency and consequently we can expect that the interactions between the alkyl chains will be reduced.

The viscoelastic properties of a monolayer derive from a balance of both lipid chain and headgroup interactions⁷⁰. It is therefore important to note that although lipid chains may contain specific structural features that should affect viscoelastic properties, the head group contributions may dominate. This situation is underscored by the particular example of POPG relative to DPPC as seen in Figure. POPG displays significantly higher viscosity values at all surface pressures above 12 mN m^{-1} than DPPC attributed to the potential for hydrogen bonding between POPG head groups which would lead to increased lipid interactions⁹⁸. At low surface pressures both DPPC and POPG are in a liquid expanded phase and show similar elasticity values. As DPPC forms a condensed phase, a distinct change in elasticity is observed. The elasticity of the

condensed phase of DPPC is observed to be much higher than that of the POPG liquid expanded phase. The measured viscoelastic properties for both lipids are within the range reported for similar lipid monolayer systems^{14,72,113}. The LS mixture monolayer displays viscosity values similar to those of DPPC, the major component, although the presence of POPG increases these values above the phase transition. The mixture exhibits elasticity values associated with a liquid expanded phase up to 20 mN m⁻¹ after which a distinct change is observed, associated with formation of the DPPC-rich condensed phase. The phase transition for the mixture is higher than that of pure DPPC due to the presence of some POPG in the condensed phase.

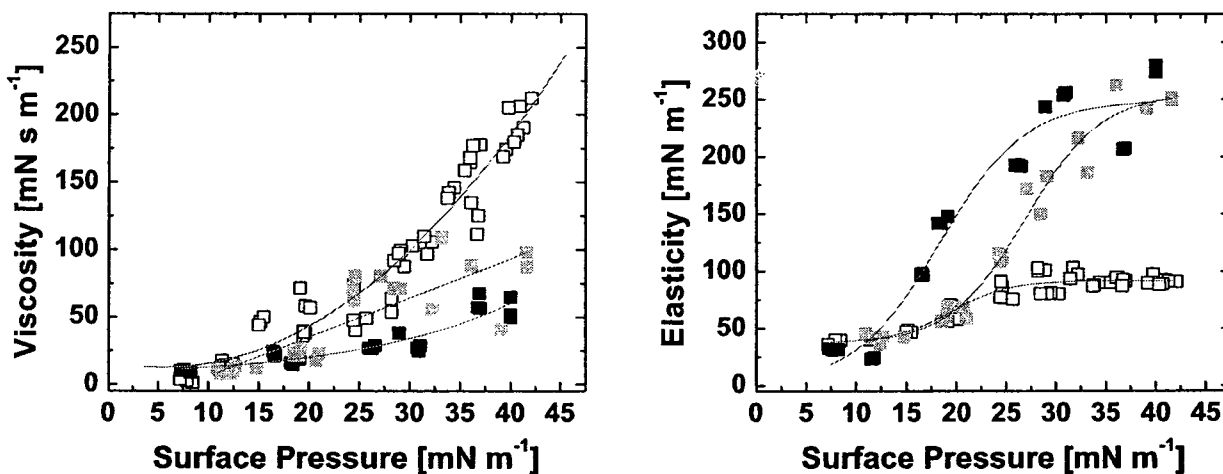


Figure 4.4. Dilational viscosity (left) and elasticity (right) of POPG (\square), DPPC (\blacksquare) and POPG/DPPC (20/80) (\blacksquare) monolayers on water at 23 °C. Trend lines are added to guide the eye only.

Oxidized and unoxidized POPG (Figure top) films exhibit similar viscosity and elasticity values up to 15 mN m⁻¹ above which they diverge and the oxidized monolayer exhibits lower values than the unoxidized monolayer. The decrease in values for both viscosity and elasticity following oxidation reflects the divergent monolayer compressibilities. These changes are a consequence of the chemical modifications of

POPG induced by ozone and the consequent lipid reorganizations. The viscosity of POPG ranges from approximately 0 to 225 mN s m⁻¹, while the oxidized POPG film has a range from approximately 0 to 125 mN s m⁻¹ at comparable surface pressures. This reduction in film viscosity may have physiological implications since the respiratory system must maintain a sufficiently high lung surfactant film viscosity to keep lung surfactant at the alveoli. In particular, the viscosity must counterbalance the surface tension gradient that acts to drive lung surfactant away from the alveoli (surface tension in the alveoli is maintained near 70 mN m⁻¹ while the surface tension in the upper airways approaches 30 mN m⁻¹)⁴². The reduction in viscosity observed here may therefore lead to a loss of lung surfactant material to the upper lung airways. The POPG monolayer exhibits elasticity values ranging from 0 to 100 mN m⁻¹ while the oxidized POPG monolayer exhibits values ranging from approximately 0 to 70 mN m⁻¹ over a comparable surface pressure range. Healthy lung surfactant composition allows the rapid re-spreading of compressed lung surfactant films as respiration occurs. The elastic parameter of these films is therefore essential to ensure efficient compression and expansion at the alveolar surface. The observed loss of elasticity due to ozone exposure may reduce the film re-spreadibility causing additional stress on the respiratory system. Overall the viscoelastic properties of POPG are significantly reduced after exposure to ozone attributed to reduced interactions within the oxidized POPG monolayer.

Figure (bottom) shows the viscosity and elasticity for the model LS mixture which contains only 20% ozone reactive component in the monolayer. The viscosity values of the mixture before and after oxidation are very similar and increase from approximately 10 to 110 mN s m⁻¹ over the surface pressure range studied. However, it

should be noted that as the surface pressure is increased beyond 20 mN m^{-1} , viscosity values become increasingly scattered. This may be due to the fact that the viscosity is more sensitive to amplitude and frequency changes in the pendant drop oscillation than elasticity^{14,78,80}. Initially, the elasticity values for the oxidized and unoxidized LS mixture are very similar, and range between 50 to 100 mN m^{-1} up to surface pressures of 25 mN m^{-1} . At 25 mN m^{-1} the values begin to diverge with the unreacted LS mixture reaching elasticity values between 240 to 260 mN m^{-1} and the oxidized monolayer only reaching 200 to 225 mN m^{-1} . Thus, the model lung surfactant monolayer exhibits a similar magnitude decrease in its elasticity, as much as 30 - 50 mN m^{-1} , when it is actually only comprised of 20% POPG. This indicates that any change in the elasticity of the reactive liquid expanded component will generate a significant effect on the elasticity of the entire film. Changes in rheological parameters are generally a consequence of changes to the lipid monolayer organization. Since the POPG is the only reactive component and it is predominantly phase separated from DPPC, these reorganizations are likely occurring within the POPG liquid expanded phase. The fact that the minor component has such a strong influence on the entire film elasticity underscores the importance of complex interactions between both components and phases in determining the rheology of the system.

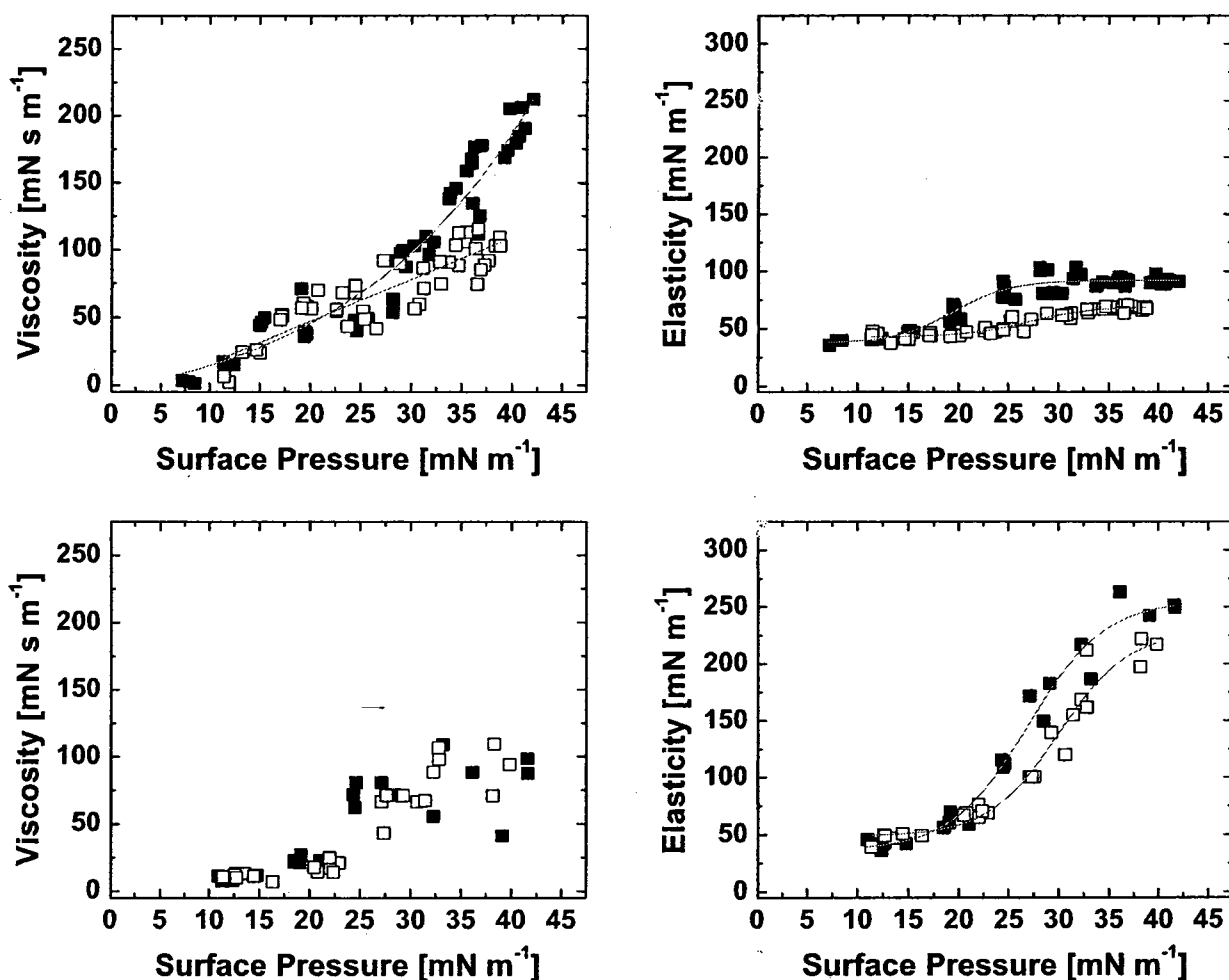


Figure 4.5. Dilational viscosity (left) and elasticity (right) of POPG (top) and POPG/DPPC (20/80) (bottom) monolayers on water at 23 °C before (■) and after (□) oxidation. Where appropriate trend lines are added to guide the eye only.

Brewster angle microscopy was utilized to image the surface morphology of the LS mixture before and after ozone exposure. The upper row in Figure represents the unreacted LS mixture and the lower row the oxidized LS mixture. In general, the BAM images show the clear formation of phase separated DPPC-rich condensed domains by 10 mN m⁻¹. As the molecular area is further reduced through 15-25 mN m⁻¹, we see an

increasing density of condensed phase material as lipids are packed closer together. Finally, by 40 mN m^{-1} we have a homogeneous condensed phase due to the coalescence of condensed domains and the expulsion of liquid expanded material from the surface.

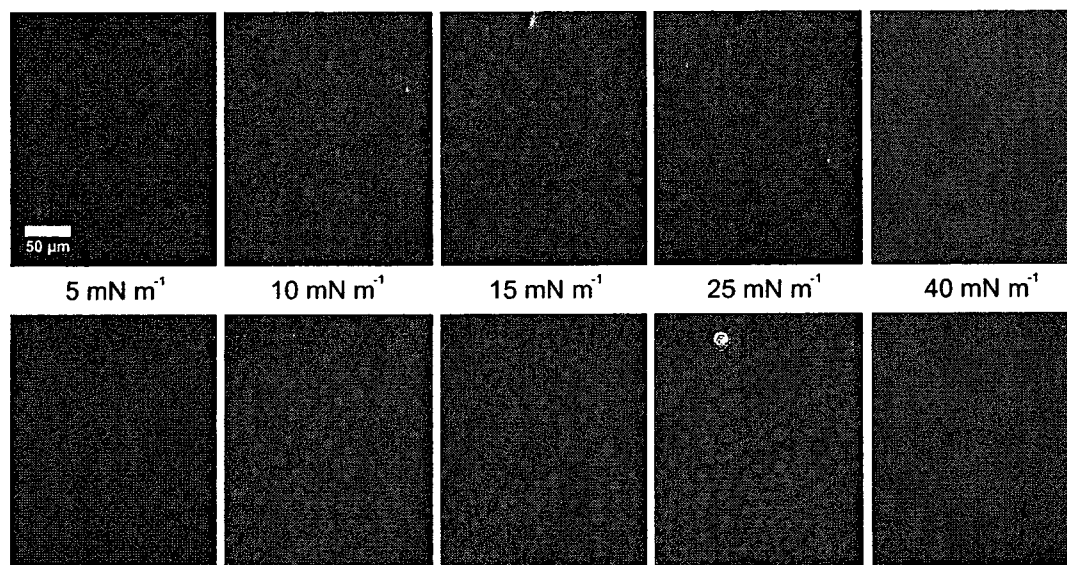


Figure 4.6. BAM images of POPG/DPPC (20/80) monolayers on water at 23 °C before (top) and after (bottom) oxidation performed on a Langmuir film balance.

The most evident difference in monolayer morphology following ozonolysis is the density of condensed phase material over the entire surface pressure range examined. The larger quantity of condensed phase material in the BAM images of the oxidized LS mixture monolayer is indicative of the greater loss of oxidized material from the surface due to higher solubility. This supports the observations noted in the recompression experiments. A homogeneous condensed phase is observed for both films indicating a loss of the liquid expanded phase⁴³ by 40 mN m^{-1} which corresponds to the collapse pressure of the POPG LE phase when the compression is performed on the Langmuir film balance. In fact, the oxidized monolayer actually shows a homogeneous condensed

phase at lower surface pressures of 30 mN m^{-1} , highlighting the increased loss of oxidized material to the bulk phase.

4.5. Conclusion

Our experimental results indicate that even after POPG and the LS mixture monolayers have been exposed to ozone they retain much of their original surface activity. However, the lipid organization is altered, evident from the isotherm shape changes, the increased solubility of products and the decreases in both film viscosity and elasticity. The lower collapse pressure of the films may be insufficient to achieve the high the surface tension reductions required to prevent collapse of the alveolar sacs. The lowered viscosity of the POPG component may also no longer balance the surface tension gradient that acts to drive lung surfactant from the lower to upper airways. The elasticity is reduced by the same magnitude in both the pure POPG and LS mixture monolayers, the latter only containing 20% reactive component. This decrease in monolayer elasticity will affect how the film recovers over the alveolar surface during exhalation, increasing the work associated with breathing. Thus ozonolysis of the pulmonary lining may affect the mechanical properties needed for normal respiration in addition to the immunogenic response reported in the literature^{12,13}. Future research will be directed at determining the role of protein oxidation on these mechanical properties and the extent of damage at different levels of ozone exposure.

Chapter 5. Surface Activity and Rheological Changes in Survanta Films Resulting from Ozone Exposure

5.1. Abstract

Survanta is a clinically used lung surfactant replacement obtained from a bovine lung lavage and consists of a mixture of phospholipids and surfactant proteins SP-B and SP-C. Survanta monolayers on a pendant drop apparatus have been used to examine the surface activity and rheological changes ozone inhalation may induce in lung surfactant. These experiments reveal that Survanta films, which include the membrane proteins, reach higher surface pressures and viscosities upon compression compared to pure lipid films. Sequential compression-expansion cycles on Survanta films show an increased loss of material to the subphase after lipid oxidation. Brewster angle microscopy (BAM) experiments have shown significant changes to Survanta film morphology following ozonolysis in the form of large aggregates, indicating changes to component interactions. Despite many of the changes in film behavior caused by ozone exposure, the rheology of the Survanta films is unchanged by the oxidation.

5.2. Introduction

Lung surfactant is a mixture of phospholipids and membrane proteins covering the alveoli which are found on the surface of our lungs^{2,3,9}. Lung surfactant prevents the collapse of the alveoli sacs, which resemble small air bubbles, by reducing the surface tension at the air-water interface⁸. Since lung surfactant represents an interface between

the exterior atmospheric environment and the interior of our bodies it must be up to task in serving several roles simultaneously. Primarily, the role of lung surfactant is to facilitate respiration, it also serves as a first defense mechanism to foreign particles³. In this protective role it is responsible for the clearing of harmful inhaled material such as bacteria, viruses, and particulate irritants from the lung surface. The biophysical function of lung surfactant films during respiration is highly dependent on the molecular structures and interactions of both the lipid and membrane protein content. Since the lung surface is a primary target of airborne pollution found in many urban environments, the functioning of lung surfactant films after exposure to pollutants may be reduced. The structures of lung surfactant constituents may be altered by certain inhaled reactive airborne chemicals^{20,30}. This can lead to detrimental effects during respiration and may increase the amount of work needed to breathe^{13,18}.

The manner in which lung surfactant functions during respiration is of particular interest not only for lung damage due to airborne pollutants, but also for cystic fibrosis and infant respiratory distress syndrome (IRDS)¹³. For each of these health concerns a component of lung surfactant is altered, non-functional or absent and respiration becomes strained for affected individuals. To address these health issues, significant lung surfactant research has focused on replacement therapies whereby supplemental lung surfactant is administered to the patient¹¹⁴. Therefore a better understanding of the component interactions in functional lung surfactant and the changes induced by environmental factors will be of great benefit for the development of improved therapeutic treatments.

Lung surfactant composition varies significantly between species yet is able to serve the same function⁷. Human lung surfactant is a mixture of approximately 90% lipid and 10% protein by weight^{28,29}. Studies have shown that 80% of the lipid content is saturated phosphatidylcholine (PC) predominantly found in the form of dipalmitoylphosphatidylcholine (DPPC)³. Another 10% of the lipid composition corresponds to phosphatidylglycerol (PG) mainly found as palmitoyloleoylphosphatidylglycerol (POPG) and the remaining 10% is comprised of smaller amounts of phosphatidic acid (PA), phosphatidylinositol (PI), phosphatidylethanolamine (PE) and cholesterol⁷. Although clearly dominated by certain saturated and unsaturated structures, natural lung surfactant contains a wide variety of lipid side chain substitutions^{28,29}.

There are four lung surfactant proteins (SP) needed to achieve proper lung surfactant functionality: SP-A, SP-B, SP-C, and SP-D^{3,7}. SP-A and SP-D have been shown to have antimicrobial properties as well as some evidence indicating a possible role in enhancing the activities of SP-B and SP-C^{3,7}. SP-B and SP-C on the other hand have been shown to have a direct role in maintaining proper mechanical functioning of the lung surfactant film through specific interactions with lipids^{8,9}. Using a variety of surface specific techniques, research has shown that varying the lipid and protein components significantly alters the surface tension, adsorption, morphology and rheological behavior of lung surfactant films^{9,80}.

The rheological behavior of lung surfactant at the alveolar surface is important as it is essentially a thin film that is repeatedly expanded and compressed during respiration. Rheology describes the stress and strain of a material or a thin lipid film when perturbed

by an applied force in terms of viscosity and elasticity¹⁴⁻¹⁶. The dilational viscosity of thin films can be related to the force needed to separate neighboring membrane molecules. Dilational elasticity describes the recovery of a film after being subjected to an applied force. Films that exhibit both viscous and elastic characteristics are said to be viscoelastic. Films with higher viscoelasticity generally consist of molecules which have strong interactions opposing intermolecular displacement and favoring the recovery of film organization¹⁴.

It is clear that lung surfactant components interact together to minimize surface tension and achieve a balance between film viscosity and elasticity^{9,80}. Lung surfactant films exhibit reduced surface tension through the incorporation of a large proportion of saturated PC lipids, which generates near zero surface tensions and prevents alveolar collapse⁸. The viscosity and elasticity of lung surfactant films keep the lipid-protein mixture at the surface of the alveolar sacs and promotes film cohesiveness during respiration^{4,42}. The dilation and contraction of lung surfactant films on the surface alveolar sacs is facilitated by a mixture of saturated/unsaturated phospholipids. Due to packing constraints unsaturated lipid films exhibit significantly greater fluidity relative to saturated lipids in a compressed state. This fluid state, called a liquid expanded (LE) phase in monolayers, will allow much more mobility within the lipid film allowing rapid re-spreading⁸.

The presence lung surfactant proteins SP-B/SP-C is essential for the normal functioning of pulmonary films during respiration^{42,62}. As breathing occurs the available molecular area at the alveoli surface is reduced eventually resulting in unsaturated lipids being 'squeezed out' from the film and into the subphase^{3,8}. The lost unsaturated lipids

are kept in close proximity to the interface as an associated bilayer through cooperative anchoring interactions with SP-B and SP-C^{4,42}. The squeezed out material is then reincorporated into the interfacial layer as the alveoli surface is expanded upon inhalation. Without the surfactant proteins, squeezed out lipid material would be irreversibly lost to the subphase. SP-B has been associated with modifying the collapse event while SP-C is thought to help maintain the anchored reservoir near the interface. The surfactant proteins have also been shown to have a role in modulating the viscosity in highly compressed films. The SP-B and SP-C surfactant proteins interact with the lipid layer through both hydrophobic and electrostatic interactions^{44,46,56}. Research using knock-out mice for both SP-B and SP-C separately have shown that mice which lack SP-B do not survive⁴⁴, and those which lack SP-C are more susceptible to respiratory problems⁴².

Certain components of lung surfactant are particularly susceptible to oxidation^{20,35,18}. In industrialized urban areas one of the most commonly encountered atmospheric oxidant sources from our environment is photochemical smog. Photochemical smog is formed when nitrogen oxides and volatile organic compounds react in sufficient UV radiation to form various toxic airborne substances. The main oxidant component in photochemical smog is ozone and it can become a health concern at atmospheric concentrations higher than 0.065 ppm according to government standardized air quality index tables¹¹⁵. Ozone concentrations greater than 0.1 ppm are considered a serious environmental health hazard. Many research groups have linked ozone inhalation to respiratory problems such as coughing or shortness of breath and also increased susceptibility to bacterial infections^{12,18}. Ozone is highly reactive and therefore will not

penetrate deeply into lung tissues³². Toxicity is further transmitted into deeper tissues through reactive oxygen species such as hydroxyl radicals, peroxides or aldehydes. Ozone is known to readily react with unsaturated lipids through the Criegee mechanism^{30, 34} as well as oxidize certain amino acid groups in proteins^{18,27}. The amino acids which have notable sensitivity towards ozone are Trp > Met > Cys >> Tyr >>>Phe²⁷.

The research presented here investigates the surface activity and dilational rheology changes generated by ozone exposure in model monolayers composed of Survanta. Survanta is a clinically used lung surfactant replacement comprising bovine lung lavages with additional DPPC, palmitic acid, and triacylglycerols. SP-A, SP-D and cholesterol have been removed²⁸. Overall it contains nearly 95% lipids in approximately a 75-25 ratio of saturated to unsaturated components as well as up to 5% surfactant proteins SP-B and SP-C^{28,29}. The saturated lipid components of Survanta are predominantly PC lipids while the unsaturated components are found as PC, PE, or PG lipids. Bovine lung surfactant contains approximately $10.9 \pm 1.1 \mu\text{g } \mu\text{mol}^{-1}$ (lipid) SP-B and $34.1 \pm 4.7 \mu\text{g } \mu\text{mol}^{-1}$ (lipid) SP-C²⁸. Survanta films contain about 10% SP-B and 50% SP-C relative to the native protein concentrations²⁸.

5.3. Methodology

Survanta was obtained in a NaCl buffer solution of 4 mg ml^{-1} from Abbott Inc. Canada. It was lyophilized overnight to ensure complete loss of the water component, and stored at $-8 \text{ }^{\circ}\text{C}$. Dipalmitoylphosphatidylcholine (DPPC), 1-palmitoyl-2-oleoyl-phosphatidylglycerol (POPG) and dioleoylphosphatidylglycerol (DOPG) are used as received (Avanti Polar Lipids, Alabaster, AL, USA; purity > 99%). The water subphase is ultrapure water (resistivity $18.2 \text{ M } \Omega \text{ cm}^{-1}$) obtained using an Easypure II LF

purification system (Barnstead, Dubuque, IA, USA). The spreading solvent used for Survanta in all experiments is a 4:1 chloroform/methanol solution. DPPC and POPG were both spread from chloroform. HPLC grade chloroform and methanol are used as received (Fisher Scientific, Pittsburgh, PA, USA).

Compression isotherms and rheological measurements are performed on a profile analysis tensiometer (PAT) (SINTERFACE Technologies, Berlin, Germany). The PAT set-up uses the visual profile of a pendant drop to determine an interfacial pressure. This analytical method is called axisymmetric drop shape analysis (ADSA)^{16,86} and applies the Young-Laplace equation relating a pendant drop curvature to the interfacial pressure⁴⁸. The PAT can be programmed to generate linear decreases or sinusoidal oscillations in pendant drop volume as is the case for compression isotherms and rheological experiments respectively. Since this method of determining surface pressure depends on a visual profile the pendant drop must maintain a Laplacian shape. Therefore the choice of oscillation frequency and amplitude are of significant importance^{14,78,80} during rheological measurements. The influence of frequency and amplitude have been previously reported^{3,80}. All rheological experiments are performed using a frequency of 0.025 s^{-1} and oscillation amplitude of 2.5% of the drop size. These parameters prevent monolayer collapse, the loss of the pendant drop from the capillary tip as well as minimizing total harmonic distortions.

Isotherms are performed on monolayers spread from a solution of 0.1 mM (approximately 0.085 mg ml^{-1}) at the surface of a 10 to 15 μL ($25 - 35\text{ mm}^2$) pendant drop of water formed at the tip of a capillary tip. The spreading volumes used to deposit Survanta on the pendant drop surface typically range between 0.4 to 0.9 μL . After

spreading the lipid solution at the drop surface it is left standing for 3 minutes to allow complete evaporation of the spreading solvent. Prior to monolayer compression the pendant drop volume is increased to 26 μL (40 mm^2), and again left for 3 minutes to allow lipid equilibration at the surface prior to compression. The surface area is decreased using a molecular compression speed of $0.13 \text{ \AA}^2 \text{ molecule}^{-1} \text{ s}^{-1}$. All experiments are performed at room temperature ($23 \text{ }^\circ\text{C}$).

Rheological experiments are performed on monolayers prepared as in isotherm experiments. The lipid monolayer is compressed to a specific target pressure at a drop size of $10 \mu\text{L}$ (20 mm^2) followed by sinusoidal oscillations of the drop surface area. A complex elastic modulus can be derived by relating the variations in surface area to the surface pressure response⁸⁶. An elastic modulus is then used to calculate the dilational viscosity and elasticity of the monolayer^{14,16,17}.

Ozonolysis of Survanta monolayers at the surface of a pendant drop is carried out by enclosing the prepared drop in a small reaction chamber with a volume of 40 mL. The enclosed drop is then exposed to ozone by filling the reaction chamber with controlled ozone concentrations. A digital mass flow controller (Aalborg, Orangeburg, NY) operating at a flow rate of 100 mL min^{-1} is used to accurately control the introduction of ozone. The ozone source is an ozone generator (UVP, Upland, CA) connected in series to an ozone monitor (2B Technology, Boulder, CO) allowing precise control of ozone concentration levels. Monolayers are exposed to ozone concentrations of approximately 8 ppm for 10 minutes after which ozone exposure was terminated as no further change in surface pressure could be observed.

The morphology of Survanta monolayers are visualized using Brewster angle microscopy (BAM) performed with an I-Elli2000 imaging ellipsometer (Nanofilm Technologies GmbH, Göttingen, Germany) The ellipsometer is equipped with a 50 mW Nd:YAG laser ($\lambda = 532$ nm). The BAM images are obtained using a 20X magnification lens with a lateral resolution of 1 μm at an incident angle of 53.15°. All BAM experiments are performed on a Langmuir film balance (NIMA Technology Ltd., Coventry, U.K.) at a compression speed of 0.09 $\text{\AA}^2 \text{ molecule}^{-1} \text{ s}^{-1}$ and at room temperature. The monolayers examined using BAM are exposed to an ozone concentration of 8 ppm with a flow rate of 100 mL min^{-1} for 30 minutes. The longer exposure time is due to the greater reaction chamber volume created by enclosing a Langmuir trough.

5.4. Results and Discussion

Ozone is detrimental to lung surfactant films as it chemically modifies the structures of both the lipid and protein components thereby changing their underlying interactions^{12, 13, 18}. These interactions between lung surfactant components are necessary for functional surface activity and viscoelastic behavior⁸. In general unsaturated lipids will react with ozone forming aldehydes, carboxylic acids, and hydroxyl hydroperoxides as the double bonds within the alkyl chains are cleaved^{30,34}. Since lipid biophysical properties at the air-water interface are directly related to their amphiphilic structure, removing a portion of the hydrophobic chain will change this behavior. Certain amino acids are also known to react with ozone²⁷ creating oxidized side chains with altered structure and/or polarity which may modify the protein structure-function relationship. Figure (left) illustrates the ozonolysis of POPG, the major unsaturated lipid component,

increases, the surface pressure is seen to decrease, indicating that certain components of Survanta, the unsaturated lipids and/or certain amino acids are susceptible to oxidation. A change in film surface pressure occurs when the monolayer experiences some form of molecular rearrangement. This could be due to a loss of surface material to the bulk phase, a chemical modification of the surface material, or a combination of both these events. Compression isotherms performed before and after ozonolysis are well suited to investigate such possible changes.

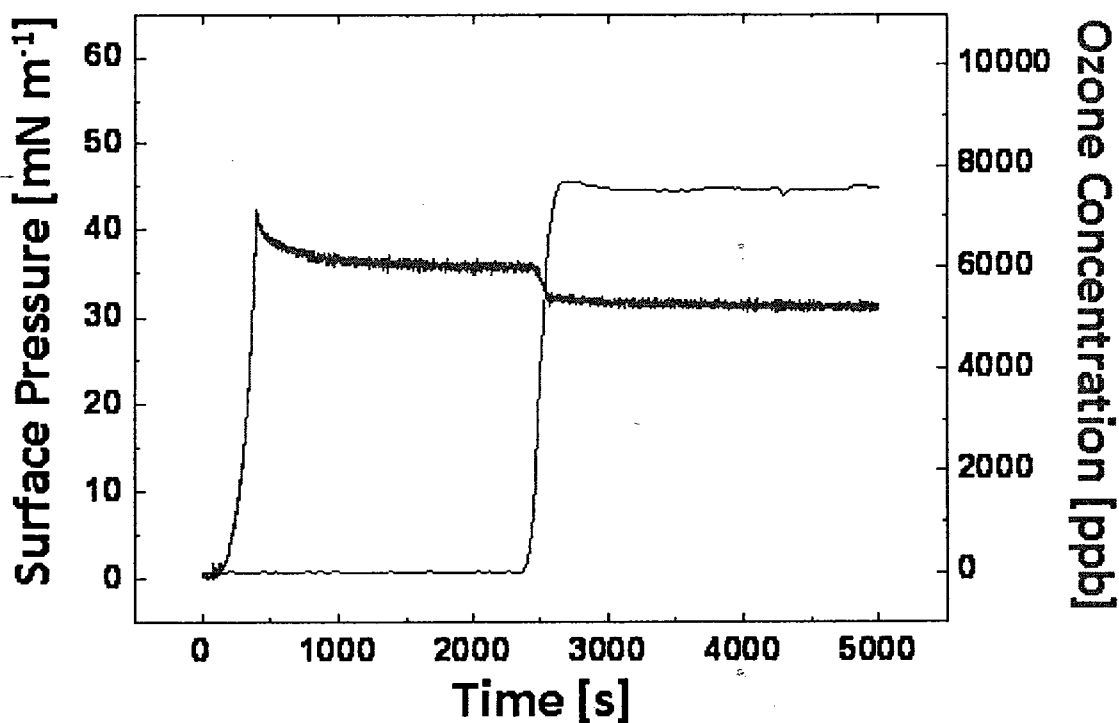


Figure 5.2. Real time changes to Survanta surface pressure during ozonolysis, illustrating the ozone sensitivity of these films. Surface pressure (—) and ozone concentration (---).

The unsaturated lipids POPG and DOPG were chosen as representative oxidation targets within the complex lipid mixture of natural lung surfactant systems. A

POPG/DPPC mixture is used to investigate the extent of monolayer changes when only one lipid component is reactive towards ozone. Survanta films represent a complete lung surfactant system in which the membrane proteins SP-B and SP-C are present. The isotherms in Figure (top) show that unreacted POPG and DOPG monolayers exhibit a liquid expanded (LE) phase until their collapse attributed to the unsaturated alkyl chains⁴⁷. This unit of unsaturation is the site of oxidation when the ozonolysis is performed, which results in the cleavage of a portion of the alkyl chain (Figure left).

POPG contains a single unsaturated chain, therefore when oxidized it retains one complete alkyl chain. A comparison between the POPG isotherms before and after ozone exposure indicates that even after losing some hydrophobic character, oxidized POPG films can still reach surface pressures greater than 40 mN m^{-1} . In fact oxidized POPG monolayers reach surface pressures only 5 mN m^{-1} lower than the unreacted POPG films. The oxidized POPG isotherms are shifted towards a greater molecular area which corresponds to a film expansion, increased surface material or a combination of both. A film expansion or rearrangement may be caused by oxidized POPG lipids now occupying more surface area as the added functional group at the site of ozone cleavage re-orientes towards the water subphase. The increased surface material could arise from the smaller cleaved fragment (nonanal or nonanoic acid) inserting at the interface through favorable chain interactions rather than being lost to the bulk.

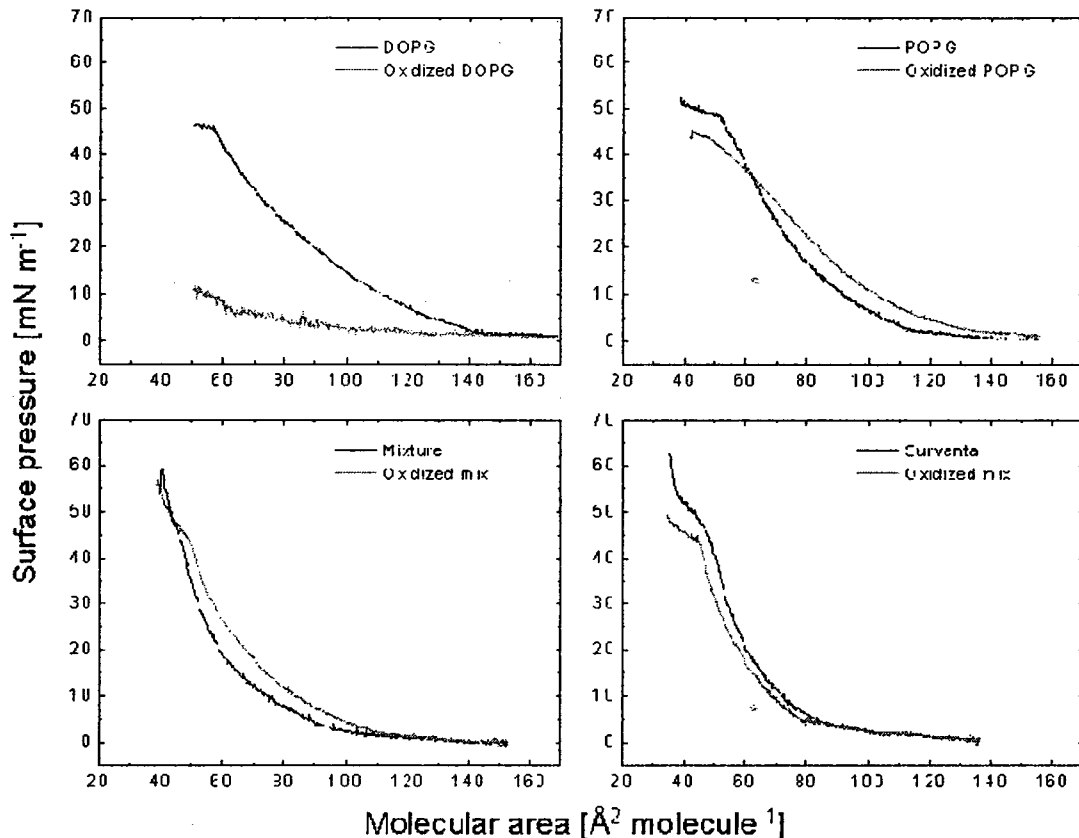


Figure 5.3. Isotherms of POPG, DOPG, POPG/PPC (20:80), and Surventa monolayers on water at 23 °C before (—) and after (---) exposure to ozone.

DOPG contains two unsaturated chains and demonstrates the effects on surface activity following cleavage in both of the lipid chains. The oxidation in this situation will remove even more of the hydrophobic portion of the lipid and the effect on surface activity should be more pronounced compared to POPG. The isotherms of DOPG before and after ozonolysis show that following oxidation the monolayer can no longer reach surface pressures over 10 mN m^{-1} when compressed to the same extent as the unreacted film corresponding to a significant increase in solubility. We can conclude that cleavage of a single alkyl chain (POPG) yields a lipid with significant surface activity but altered

film organization whereas cleavage of both chains (DOPG) results in a loss of much of the surface activity.

Mixtures of POPG/DPPC (20:80) were previously investigated to determine the changes to surface activity when only one component of a mixture is susceptible to oxidation (Figure 3.2 and Figure from Chapter 4). Isotherms of these mixtures were noted to have approximately the same relative increase in molecular areas as pure POPG films following exposure to ozone. This is significant since the mixture monolayer only contains 20 % reactive component. The mixture film, like POPG also retains much surface activity after oxidation. The isotherm shift to greater molecular areas is attributed to the same possibilities as for pure POPG films. A kink in the isotherm at higher surface pressures was attributed the collapse of oxidized POPG material. This work is of particular interest as a comparison to oxidized Survanta films as it serves as a general model for lung surfactant behavior without the inclusion of membrane proteins. Survanta lipid content comprises approximately 75% saturated PC and up to 25% unsaturated components.

Survanta isotherms reach the highest surface pressure of any of the examined lipid monolayers (Figure) attributed to the presence of the lung surfactant proteins. This large reduction in surface tension is essential for a good lung surfactant replacement to prevent the collapse of the alveoli. The kink at higher surface pressures corresponds to the collapse of unsaturated material from the monolayer as seen in the POPG/DPPC mixture. The collapse of the unsaturated lipids corresponds to the squeeze out event known to occur in lung surfactant films during respiration. Reacted Survanta films show reduced surface pressure compared to the unreacted films after the same extent of compression.

This indicates that Survanta films contain ozone sensitive unsaturated lipids and/or protein components. In contrast to the POPG/DPPC mixture isotherm results, following oxidation the Survanta films exhibit a shift to smaller molecular areas which indicates a film contraction or loss of material from the surface. In terms of composition the significant differences between the POPG/DPPC mixture and Survanta are the lipid composition and the inclusion of surfactant proteins. The lipid composition is known to be predominantly DPPC and POPG, though it also contains a small portion of polyunsaturated lipids such as DOPG which contains two unsaturated chains. The small portion of polyunsaturated material will lose a significant amount of surface activity as seen in the DOPG isotherms after ozonolysis. This material will be easily lost to the subphase and lead to the observed film contraction.

Alternatively, the observed contraction may be linked to oxidation induced changes in the SP-B and SP-C proteins, which may lead to altered interactions between the lipids and surfactant proteins. Many protein experiments have shown that substitution of different residues or mutations in the amino acid sequence can generate significant structural changes¹¹⁶. The oxidation of residues within membrane proteins will similarly result in protein structure changes or partial unfolding^{18,117,118}. Oxidation of amino acids creates localized polar environments which will alter protein interactions with the lipid film. Ensuing structural changes could alter the orientation of the protein at the interface leading to modified molecular area requirements. Computer modeling of both the SP-B and SP-C proteins has shown the positions of several surface exposed residues susceptible to oxidation (Figure). These residues are predominantly cysteines (red), methionines (orange) and tryptophans (blue). The position of ozone sensitive residues on

the surface of the protein indicates that ozone exposure has the potential of directly disrupting lipid-protein interactions.

Experiments using lung surfactant exposed to oxidants such as environmental tobacco smoke (ETS), confirmed the loss of helical structures in both proteins using FTIR measurements¹⁸. This group also observed the specific degradation of Trp and Tyr residues via a reduction of fluorescence emission. Confirmation of amino acid oxidation upon ETS exposure in both SP-B and SP-C was obtained using MS. Furthermore, the mass change in reacted SP-C was noted to additionally correspond to the loss of palmitoyl chains at the cystein residues (Figure)^{18,118}. These chains are known to interact with lipid chains during respiration and stabilize the protein orientation. As SP-C is the main protein component in Survanta the loss of palmitoyl chains may be linked to the observed film contraction.

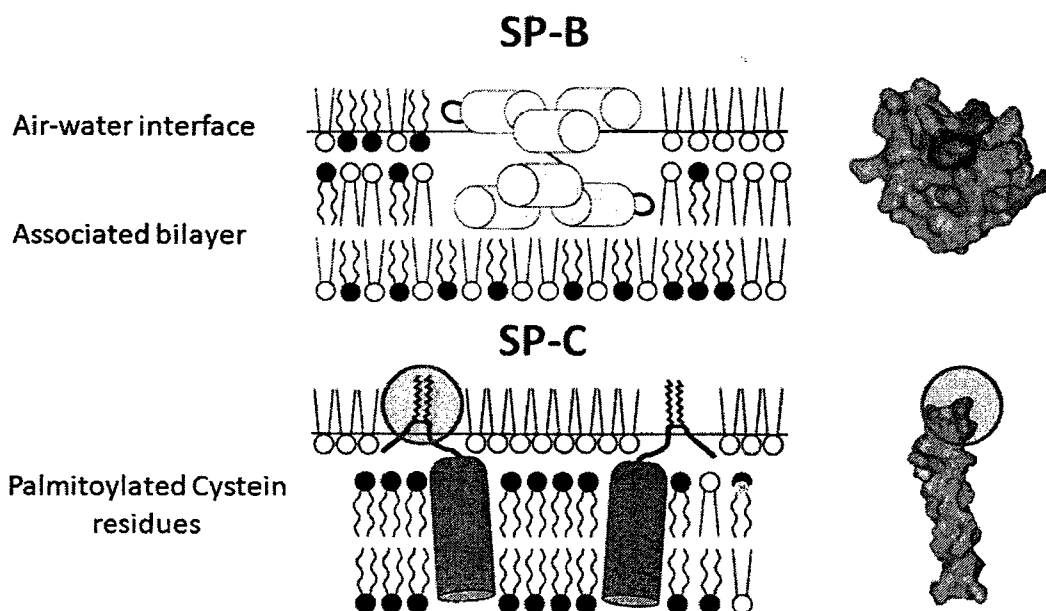


Figure 5.4. Model protein images (Pymol) showing ozone sensitive surface exposed residues and the protein orientation within the lipid membrane (modified from³).

Isotherm results indicate that the oxidation of lipid and Surfactant films modifies the interactions occurring at the interface. These changes at the interface have been investigated using BAM to image the film morphology following ozonolysis (Figure). Surfactant monolayers are compressed and the images are taken at increasing surface pressures either before or after ozone exposure. The condensed phase in BAM corresponds to the brighter regions and the LE phase is shown as the darker regions. Before oxidation, Surfactant films exhibit phase separation of LE and condensed phases at all surface pressures. The condensed phase domains show a relatively consistent size distribution as surface pressure is increased. A comparison of similar BAM experiments on a POPG/DPPC mixture noted that by 35 mN m^{-1} only a condensed phase was present (Figure from Chapter 4). This highlights the role SP-B and SP-C serve in terms of

anchoring the LE component at the surface as seen in the Survanta film images. When these proteins are not present as in the POPG/DPPC mixture, the LE components are completely expelled and irreversibly lost to the subphase⁵⁶.

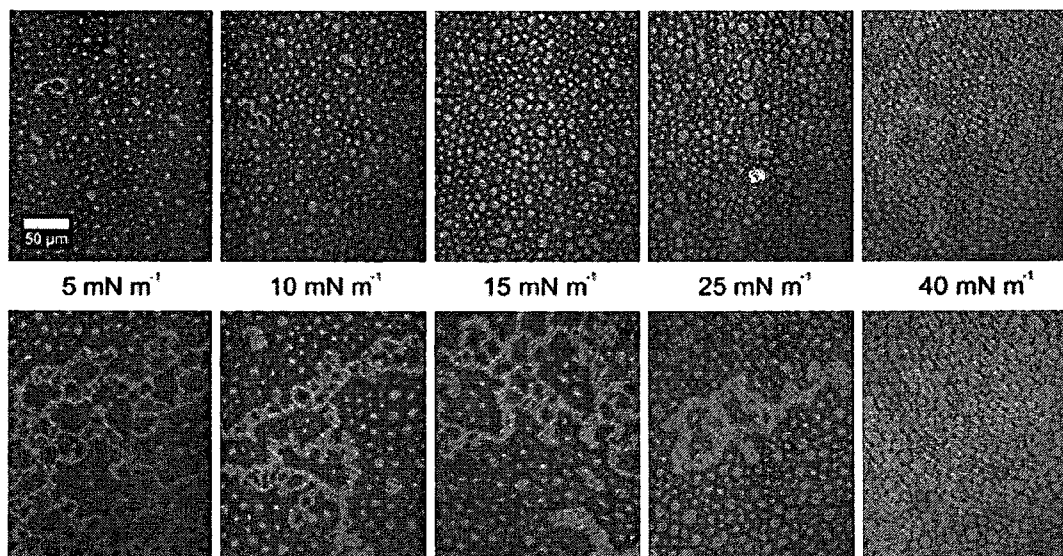


Figure 5.5. BAM images of Survanta monolayers on water at 23 °C before (top) and after (bottom) oxidation performed on a Langmuir film balance.

Following oxidation the Survanta film exhibits significant changes to film morphology in the form of large aggregates among the regular domain shapes. Aggregates are seen at surface pressures as low as 5 mN m⁻¹ and persist to approximately 40 mN m⁻¹. These morphological changes were not observed in films consisting only of POPG/DPPC (20:80) mixtures, therefore the aggregate formation is attributed to the presence of the surfactant proteins. As shown in the molecular modeling of the two surfactant proteins (Figure), some of the oxidative changes induced in the protein structure will occur on their surfaces. These aggregate species may be a result of new protein interactions generated at their surface between each other or with the lipid components. Furthermore, the film contraction observed in the isotherms may be related

to the formation of aggregates at the interface, as the greater density of condensed phase material at similar surface pressures before and after oxidation corresponds with the loss of unsaturated material from the surface.

Film solubility in the water subphase before and after oxidation was examined by performing recompression experiments on monolayer films. In these experiments, a monolayer was spread on the surface of a pendant drop and then subjected to 5 compression-expansion cycles. These experiments were performed on reacted and unreacted POPG, the POPG/DPPC mixture, and Survanta. For unreacted POPG (Figure) it was noted that each subsequent compression cycle produces a shift to smaller molecular areas. This indicates that as the monolayer is compressed and expanded some of the lipids dissolve into the bulk phase and the ensuing re-adsorption is slow^{45,56,63,119}. The greatest loss of POPG monolayer material occurs between the first three recompression cycles where a steady shift in the isotherms is observed. Similar experiments have also found the greatest loss of material to the bulk phase occurs between the first compression cycles^{4,19}. Subsequent recompressions cycles exhibit a negligible loss of monolayer material indicating a solubility limit for POPG in the bulk phase. The reacted POPG monolayer (Figure) displays a significantly greater loss of surface material to the subphase when subjected to the same recompression experiments. This conclusion is based on the larger shifts observed between all compression cycles. Compared to the POPG experiment, the reacted monolayer does not reach a solubility limit in bulk phase as rapidly, again indicating a greater loss of surface material to the bulk phase with the increased hydrophilicity.

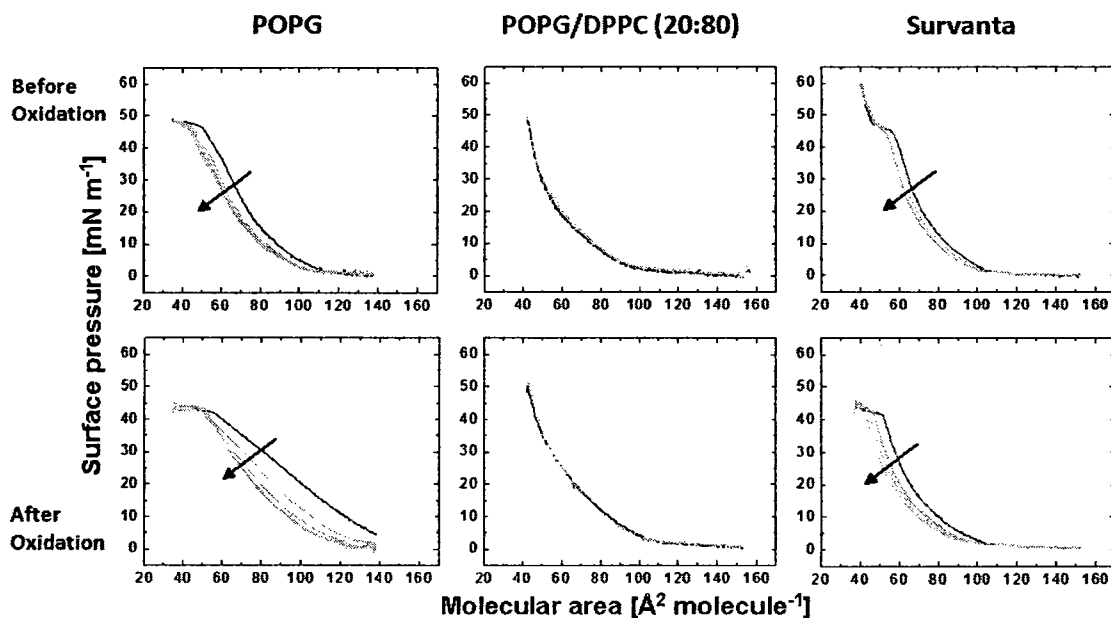


Figure 5.6. Recompressions of POPG, POPG/DPPC (20:80), and Survanta before (top) and after (bottom) ozone exposure. Monolayers are compressed and expanded for a total of 5 cycles. The black line corresponds to the first compression, consequent compressions are shown in grey with the arrow indicating the direction of isotherm shifts as material is lost from the surface.

The POPG/DPPC mixture (Figure) does not demonstrate a noticeable shift to reduced molecular areas during isotherm cycling. This is attributed to the high proportion of insoluble, saturated lipids which may mask the loss of POPG (oxidized or unoxidized). Additionally, the interactions between the saturated and unsaturated components might reduce the loss of material to the subphase. Only the first two compression cycles are shown as subsequent cycles are identical.

The Survanta monolayers (Figure) show small shifts towards lower molecular areas as the compression cycles occur, indicating a loss of material to the bulk phase. The greatest shifts in isotherms occur between the first three compression cycles, subsequent isotherm compressions after this point are no longer shifted to lower molecular areas.

These results are similar to the pure POPG film recompressions which indicated a loss of material to the bulk phase prior to oxidation. The material lost to the subphase in the Survanta compression experiments is also likely unsaturated lipid content. However, Survanta is a mixture of up to 25% mono/poly unsaturated lipids and 75% DPPC. Therefore, it may be that the monounsaturated POPG remains at the surface through interactions with the proteins or DPPC and that the material being lost comes from the polyunsaturated components. Reacted Survanta monolayers (Figure) exhibit significantly larger shifts to lower molecular areas compared to the results before ozone exposure. The same result was observed in the pure POPG films after oxidation. This shows that after oxidation of POPG and certain components of Survanta, the films are much more soluble due to the chemical modification.

Rheological changes to Survanta monolayers induced by ozonolysis have been measured and compared to previously published results of POPG/DPPC (20:80) mixtures (Figure from Chapter 4). A comparison before oxidation of the POPG/DPPC mixture and Survanta (Figure), which have similar lipid compositions, indicates that Survanta films reach a higher viscosity at pressures above 30 mN m^{-1} . This suggests that during the film oscillations the surfactant proteins interact with the monolayer in such a way that viscosity is greatly enhanced. This is an important property of lung surfactant in order to keep it at the alveolar surface during respiration. Increased viscosity can be attributed to two factors. The first involves jamming of condensed phase domains which would restrict their flow upon significant expulsion of the LE phase. The second factor^{4,42} derives from the anchoring of the associated bilayer to the overlying film by the protein which occurs at high pressures. This coupling of the layers requires that they move in

concert hindering flow. The elasticity of Survanta films is similar to that of the POPG/DPPC mixture, which is likely due to both films containing comparable amounts of DPPC. Furthermore, the fact that elasticity is similar in the two films indicates that the proteins do not greatly influence the film elasticity and that this property is linked to lipid-lipid interactions.

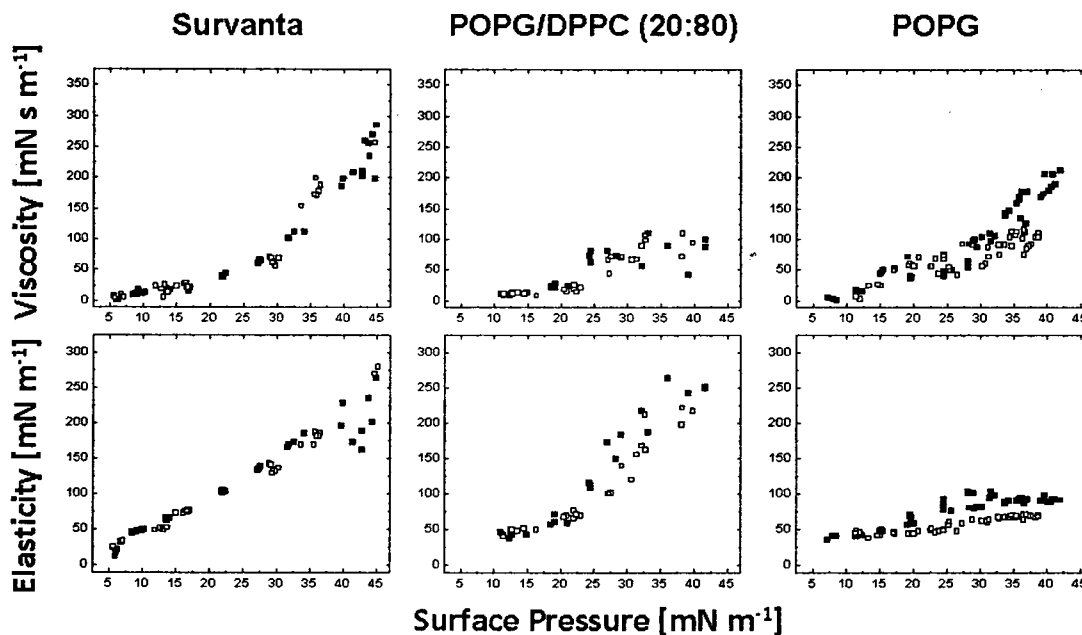


Figure 5.7. Rheological measurements of Survanta, POPG/DPPC (20:80) and POPG monolayers on water at 23 °C before (■) and after (□) oxidation.

Most significant from the rheological measurements is the fact that viscosity and elasticity of lung surfactant films does not appear to change after exposure to ozone. This is in contrast to the changes observed in the lung surfactant surface activity, morphology and recompression data after oxidation. These results are also in contrast with the confirmed changes in protein structure due to oxidation seen by other researchers which are known to alter film interactions^{18,117,118}. The data presented here indicates that lipid

and protein interactions are disrupted by oxidation, however these changes do not appear to be detrimental to all measured surface properties. The reduced maximum surface pressure and loss of material to the subphase will adversely affect the lung surfactant system. The overall rheological behavior of these films remains unchanged under the oxidative conditions employed in our study.

5.5. Conclusion

Isotherm results show that of all films examined Survanta is able to achieve the highest surface pressures, which is needed for functional lung surfactant. Following oxidation the maximum attainable surface pressure is reduced in Survanta films. The reduction in maximum surface pressure increases the work of breathing and may lead to alveolar collapse.

The lipid monolayers which contain POPG all show a film expansion upon oxidation as determined through isotherm compressions. This film expansion has been attributed to a reorganization of the oxidized film components which retain significant surface activity. Survanta films exhibit a film contraction when examined under the same ozone conditions. This is likely linked to the lipid composition of Survanta which contains mono and polyunsaturated lipids similar to the DOPG example presented. These polyunsaturated lipids have a significantly greater loss in surface activity following ozone exposure and are lost to the water subphase, leading to a film contraction. Furthermore, the film contraction may also be influenced in part by oxidized surfactant proteins which may exhibit modified film interaction and orientation. The BAM images have confirmed the changes to the Survanta film morphology following oxidation seen and indicate that

material is lost to subphase. Recompression experiments showing increased solubility following ozonolysis are in good agreement with the BAM conclusions.

The cleavage of unsaturated lipids, which are known to increase the film fluidity, increases the work required for normal breathing. This is seen in the decreased viscoelastic measurements of oxidized POPG and the decreased elasticity of oxidized POPG/DPPC mixtures. In spite of the isotherm, recompression, and morphological changes, Survanta films do not show any significant change in rheological behavior before and after oxidation. Therefore, even the altered structures of SP-B and SP-C are able to promote normal film rheology in the presence of oxidized unsaturated lipids. This observation suggests that LS protein structure may be a result of a robust structure as a defence towards oxidative stress.

Chapter 6. Conclusions

The focus of the research we have outlined was to determine the consequences of ozone exposure with respect to the impact on the biophysical properties of lung surfactant. As a starting point in this analysis the individual lipid components comprising lung surfactant were thoroughly investigated in terms of their surface activity and dilational rheology. These initial results indicated that with respect to viscoelasticity, the viscosity of a lipid film is dominated by head group interactions while elasticity is dominated by chain interactions. The difference in rheological measurements between the PC and PG lipids has been attributed to the capacity for hydrogen bonding in the PG head group. This hydrogen bonding can occur between the PG head groups or with the water subphase and in particular increases the viscosity of PG films. The greater viscosity of PG films is likely a result of the greater inter-lipid attraction or an anchoring effect between the head group and the water subphase which both oppose dilational flow at the surface. The slightly lower PG elasticity also correlates back to the hydrogen bonding effects as hydrogen bonding with the water subphase increases the head group hydration, effectively pulling PG head groups deeper into the bulk. This reduces the length of alkyl chain which can form stabilizing interactions leading to higher elasticity. This information is important for the interpretation many model lung surfactant films which are comprised of POPG/DPPC (20:80) mixtures.

A comparison of the individual POPG and DPPC film viscoelastic results to our model POPG/DPPC lipid film shows values which indicate contributions from both lipid components. The POPG/DPPC mixture exhibits viscoelastic results dominated by DPPC

but influenced by the POPG component. The addition of the POPG component is shown to proportionally increase the mixture viscosity and decrease elasticity relative to a pure DPPC film. The inter-lipid and lipid-subphase hydrogen bonding interactions of POPG generate these changes to viscoelasticity. Mixed lipid monolayers behave as a continuous cohesive layer, therefore changes to one component are felt through-out the entire system and as we have shown, the overall film rheology is modified.

This series of experiments have also shown specific changes in film biophysical properties following ozone exposure. Ozone is known to cleave the unsaturated components of lung surfactant^{13,20} such as POPG. Our experiments have successfully shown that upon cleavage of the unsaturated alkyl chain in POPG films, the surface activity and viscoelasticity both decrease. Surface activity changes were observed in both pure POPG and mixed POPG/DPPC films attributed to the isotherm shifts to greater molecular areas. The film morphology was also noted to be effected by the oxidation. Compared to the unreacted film the oxidized film exhibited a greater density of condensed phase indicating a loss of surface material to the bulk phase likely reacted POPG. The viscosity of POPG/DPPC mixtures was not significantly altered by ozone exposure but the elasticity of these films was actually decreased to the same extent as pure POPG films. This can be correlated to the initial observation that viscosity is linked to head group structure and elasticity to the lipid side chains. The structural changes induced by oxidation are in the lipid side chains therefore the mixture film elasticity is more affected than the viscosity as shown in the data.

Any changes to POPG film viscosity have been linked to changes in the film organization which modifies inter-lipid and lipid-subphase head group interactions.

Therefore the decrease in POPG film viscosity may be correlated to the observed film expansion which distances and reduces cohesive inter-lipid head group interactions. When POPG is part of a mixture such as POPG/DPPC the viscosity of the film is not affected by ozonolysis. In POPG/DPPC mixtures reacted POPG has the possibility of interacting with intact neighboring DPPC lipids. This favorable interaction may reduce or compensate for any film re-organization that would normally occur in a pure POPG film.

The comparison of pure lipid to Survanta films has shown that the inclusion of surfactant proteins SP-B and SP-C significantly modifies film behavior. The Survanta films reach the highest observed surface pressures and exhibit the greatest viscosity at high pressures as is required in their physiological role. Survanta films were shown to have both surface activity and film morphology changes following ozone exposure. This has been linked to ozone sensitive unsaturated lipid components as well as the changes oxidation will induce in certain amino acid residues within the surfactant proteins^{18,27}. The parameters of viscosity and elasticity describe the dynamic behavior of lung surfactant at the surface of the alveoli as respiration. These parameters originate from intermolecular interactions which also determine the observed surface activity and film morphology. Most significant from this research is the fact that chemical modifications which affect surface activity and film organization do not necessarily affect the film rheology as well. This observation seems to be linked to the presence of the hydrophobic surfactant proteins SP-B and SP-C. In the pure lipid films we see changes to surface activity, film behavior and rheology following ozone exposure, where as with the proteins present film rheology remains unchanged under these conditions. In spite of lipid

component and tertiary structural changes due to oxidation these proteins can continue to function and generate normal film rheology.

Our results have shown that ozone damages lipids and may affect proteins found in lung surfactant with respect to both surface activity and morphology. Individuals exposed to a high concentration of ozone for even a brief period of time experience increased work necessary for breathing. It can be concluded that exposure to high ozone concentrations can be detrimental to health not only from deep tissue damage but also from a biophysical function perspective as the mechanical properties of lung surfactant are affected.

Future challenges for understanding the biophysical changes to lung surfactant following oxidation will be determining how both lipid and protein interactions are modified. The squeeze out event occurring at high surface tensions is highly dependent on orientational based interactions between the lipids and surfactant proteins. Knowing the specific orientation of the proteins before and after oxidation would contribute to understanding how rheology appears to be unaffected even as the maximum attainable surface pressures of oxidized films decreases. Furthermore, the location and orientation of lipids following oxidation also remains to be determined. These properties may require techniques involving surface specific spectroscopic analysis such as infrared reflection adsorption spectroscopy (IRRAS). AFM measurements of oxidized films would also determine if the squeezed out reservoir material reaches the same relative thickness as the unreacted films. Experiments focusing on manipulation of the protein sequence could elucidate which portions of the proteins are essential for normal functioning and how they relate to the portions that are oxidized. Rheological and oxidation studies of these

films at biologically relevant temperatures would also be important. While at higher temperatures the LE-C phase transition of DPPC is shifted to higher pressures, at 37 °C a condensed phase is still formed⁴⁷. The influence of temperature on membrane viscoelasticity needs to be investigated. Overall, as is seen from the extensive literature on lung surfactant related topics there remain a number of unexplored issues to address ranging from therapeutic advancements to environmental health effects.

Chapter 7. References

1. Bernhard, W.; Haagsman, H. P.; Tschernig, T.; Poets, C. F.; Postle, A. D.; Van Eijk, M. E.; Von Der Hardt, H., *Am. J. Respir. Cell Mol. Biol.* **1997**, *17* (1), 41-50.
2. Bernhard, W.; Hoffmann, S.; Dombrowsky, H.; Rau, G. A.; Kamlage, A.; Kappler, M.; Haitzma, J. J.; Freihorst, J.; Von der Hardt, H.; Poets, C. F., *Am. J. Respir. Cell Mol. Biol.* **2001**, *25* (6), 725-731.
3. Veldhuizen, E. J.; Haagsman, H. P., *Biochim. Biophys. Acta* **2000**, *1467* (2), 255-70.
4. Alonso, C.; Alig, T.; Yoon, J.; Bringezu, F.; Warriner, H.; Zasadzinski, J. A., *Biophys. J.* **2004**, *87* (6), 4188-4202.
5. Halliday, H. L., *J. Perin.* **2008**, *28 Suppl 1*, S47-56.
6. West, J. F., *Respiratory physiology-- the essentials*. Williams & Wilkins: Baltimore, 1994.
7. Batenburg, J. J.; Haagsman, H. P., *Prog. Lipid Res.* **1998**, *37* (4), 235-276.
8. Zasadzinski, J. A.; C. Alonso, J. D., F. Bringezu, H. Warriner, T. Alig, S. Steltenkamp, A.J. Waring, Relationships Between Surface Viscosity, Monolayer Phase Behavior, and the Stability of Lung Surfactant Monolayers In *Structure and Dynamics of Membranous Interfaces*, Nag, K., Ed. Wiley: Hoboken, NJ, 2008.
9. Zasadzinski, J. A.; Ding, J.; Warriner, H. E.; Bringezu, F.; Waring, A. J., *Curr. Opin. Colloid Interface Sci.* **2001**, *6* (5,6), 506-513.
10. Nikischin, W.; Gerhardt, T.; Everett, R.; Bancalari, E., *Am. J. Respir. Crit. Care Med.* **1998**, *158* (4), 1052-60.

11. Putman, E.; Liese, W.; Voorhout, W. F.; Van Bree, L.; Van Golde, L. M. G.; Haagsman, H. P., *Toxicol. Appl. Pharmacol.* **1997**, *142* (2), 288-296.
12. Mudway, I. S.; Kelly, F. J., *Mol. Aspects Med.* **2000**, *21* (1-2), 1-48.
13. Ciencewicky, J.; Trivedi, S.; Kleeberger, S. R., *J. Allergy Clin. Immunol.* **2008**, *122* (3), 456-468.
14. Vrânceanu, M.; Winkler, K.; Nirschl, H.; Leneweit, G., *Colloids Surf., A* **2007**, *311* (1-3), 140-153.
15. Anton, N.; Saulnier, P.; Boury, F.; Foussard, F.; Benoit, J.-P.; Proust, J. E., *Chem. Phys. Lipids* **2007**, *150* (2), 167-175.
16. Loglio, G.; Pandolfini, P.; Miller, R.; Makievski, A. V.; Ravera, F.; Ferrari, M.; Liggieri, L., Drop and Bubble Shape Analysis as a Tool for Dilational Rheological Studies of Interfacial Layers. In *Novel Methods to Study Interfacial Layers*, Möbius, D.; Miller, R., Eds. Elsevier: Amsterdam, Netherlands, 2001; Vol. 11, pp 439-483.
17. Miller, R.; Sedev, R.; Schano, K. H.; Ng, C.; Neumann, A. W., *Colloids Surf.* **1993**, *69* (4), 209-16.
18. Stenger, P. C.; Alonso, C.; Zasadzinski, J. A.; Waring, A. J.; Jung, C.-L.; Pinkerton, K. E., *Biochim. Biophys. Acta, Biomembr.* **2009**, *1788* (2), 358-370.
19. Bringezu, F.; Pinkerton, K. E.; Zasadzinski, J. A., *Langmuir* **2003**, *19* (7), 2900-2907.
20. Pryor, W. A.; Squadrito, G. L.; Friedman, M., *Free Radical Biol. Med.* **1995**, *19* (6), 935-41.

21. Sadanaga, Y.; Matsumoto, J.; Kajii, Y., *J. Photochem. Photobiol., C* **2003**, *4* (1), 85-104.
22. Gomez, A. L.; Lewis, T. L.; Wilkinson, S. A.; Nizkorodov, S. A., *Environ. Sci. Technol.* **2008**, *42* (10), 3582-3587.
23. Wang, Q. g.; Han, Z.; Wang, T.; Zhang, R., *Sci. Total Environ.* **2008**, *395* (1), 41-49.
24. Rabl, A.; Eyre, N., *Environ. Int.* **1998**, *24* (8), 835-850.
25. Oguejiofor, G. C., *Energy Sources, Part A* **2008**, *30* (13), 1179-1188.
26. Howard, C. J.; Yang, W.; Green, P. G.; Mitloehner, F.; Malkina, I. L.; Flocchini, R. G.; Kleeman, M. J., *Atmos. Environ.* **2008**, *42* (21), 5267-5277.
27. Cataldo, F., *Polym. Degrad. Stab.* **2003**, *82* (1), 105-114.
28. Bernhard, W.; Mottaghian, J.; Gebert, A.; Rau, G. A.; von Der, H. H.; Poets, C. F., *Am. J. Respir. Crit. Care Med.* **2000**, *162* (4 Pt 1), 1524-33.
29. Rüdiger, M.; Tölle, A.; Meier, W.; Rüstow, B., *Am. J. Physiol.* **2005**, *289* (5, Pt. 1), L896.
30. Santrock, J.; Gorski, R. A.; O'Gara, J. F., *Chem. Res. Toxicol.* **1992**, *5* (1), 134-41.
31. Criegee, R., *Angew. Chem.* **1975**, *87* (21), 765-71.
32. Langford, S. D.; Bidani, A.; Postlethwait, E. M., *Toxicol. Appl. Pharmacol.* **1995**, *132* (1), 122-30.
33. Uppu, R. M.; Cueto, R.; Squadrito, G. L.; Pryor, W. A., *Arch. Biochem. Biophys.* **1995**, *319* (1), 257-66.
34. Pryor, W. A.; Church, D. F., *Oxid. Damage Repair, [Int. Soc. Free Radical Res. Bienn. Meet.], 5th* **1991**, 496-504.

35. Salgo, M. G.; Cueto, R.; Pryor, W. A., *Free Radical Biol. Med.* **1995**, *19* (5), 609-16.
36. Sanhueza, P. A.; Reed, G. D.; Davis, W. T.; Miller, T. L.; Smith, S. M., *Clean Technol. Environ. Policy* **2002**, *4* (2), 79-86.
37. Uhlson, C.; Harrison, K.; Allen Corrie, B.; Ahmad, S.; White Carl, W.; Murphy Robert, C., *Chem. Res. Toxicol.* **2002**, *15* (7), 896-906.
38. Henneberger, P. K.; Olin, A.-C.; Andersson, E.; Hagberg, S.; Torén, K., *Chest* **2005**, *128* (4), 3028-3037.
39. Triche, E. W.; Gent, J. F.; Holford, T. R.; Belanger, K.; Bracken, M. B.; Beckett, W. S.; Naeher, L.; McSharry, J.-e.; Leaderer, B. P., *Environ. Health Perspect.* **2006**, *114* (6), 911-916.
40. Kanofsky, J. R.; Sima, P., *J. Biol. Chem.* **1991**, *266* (14), 9039-42.
41. Kelly Frank, J., *Occup. Environ. Med.* **2003**, *60* (8), 612-6.
42. Alonso, C.; Waring, A.; Zasadzinski, J. A., *Biophys. J.* **2005**, *89* (1), 266-273.
43. Bringezu, F.; Ding, J.; Brezesinski, G.; Zasadzinski, J. A., *Langmuir* **2001**, *17* (15), 4641-4648.
44. Bringezu, F.; Ding, J.; Brezesinski, G.; Waring, A. J.; Zasadzinski, J. A., *Langmuir* **2002**, *18* (6), 2319-2325.
45. Ding, J.; Takamoto, D. Y.; Von Nahmen, A.; Lipp, M. M.; Lee, K. Y. C.; Waring, A. J.; Zasadzinski, J. A., *Biophys. J.* **2001**, *80* (5), 2262-2272.
46. Ding, J.; Doudevski, I.; Warriner, H. E.; Alig, T.; Zasadzinski, J. A.; Waring, A. J.; Sherman, M. A., *Langmuir* **2003**, *19* (5), 1539-1550.
47. Cevc, G., *Phospholipids handbook*. Marcel Dekker Inc.: New York, 1993.

48. Möbius, D.; Miller, R., *Novel Methods to Study Interfacial Layers*. Elsevier: Amsterdam, Netherlands, 2001; Vol. 11, p 521.
49. Johansson, J.; Curstedt, T., *Eur. J. Biochem.* **1997**, *244* (3), 675-693.
50. Goerke, J., *Biochim. Biophys. Acta, Mol. Basis Dis.* **1998**, *1408* (2-3), 79-89.
51. Sano, H.; Kuroki, Y., *Mol. Immunol.* **2005**, *42* (3), 279-287.
52. Wang, G.; Umstead, T. M.; Phelps, D. S.; Al-Mondhiry, H.; Floros, J., *Environ. Health Perspect.* **2002**, *110* (1), 79-84.
53. LeVine, A. M.; Lotze, A.; Stanley, S.; Stroud, C.; O'Donnell, R.; Whitsett, J.; Pollack, M. M., *Crit. Care Med.* **1996**, *24* (6), 1062-7.
54. Noah Terry, L.; Murphy Paula, C.; Alink Jorien, J.; Leigh Margaret, W.; Hull William, M.; Stahlman Mildred, T.; Whitsett Jeffrey, A., *Am. J. Respir. Crit. Care Med.* **2003**, *168* (6), 685-91.
55. Baatz, J. E.; Elledge, B.; Whitsett, J. A., *Biochemistry* **1990**, *29* (28), 6714-20.
56. Takamoto, D. Y.; Lipp, M. M.; von Nahmen, A.; Lee, K. Y.; Waring, A. J.; Zasadzinski, J. A., *Biophys. J.* **2001**, *81* (1), 153-69.
57. Morrow, M. R.; Taneva, S.; Simatos, G. A.; Allwood, L. A.; Keough, K. M. W., *Biochemistry* **1993**, *32* (42), 11338-44.
58. Pastrana-Rios, B.; Taneva, S.; Keough, K. M. W.; Mautone, A. J.; Mendelsohn, R., *Biophys. J.* **1995**, *69* (6), 2531-40.
59. Klein, J. M.; Thompson, M. W.; Snyder, J. M.; George, T. N.; Whitsett, J. A.; Bell, E. F.; McCray, P. B., Jr.; Noguee, L. M., *J. Pediatr. (St. Louis)* **1998**, *132* (2), 244-248.

60. Tokieda, K.; Whitsett, J. A.; Clark, J. C.; Weaver, T. E.; Ikeda, K.; McConnell, K. B.; Jobe, A. H.; Ikegami, M.; Iwamoto, H. S., *Am. J. Physiol.* **1997**, *273* (4, Pt. 1), L875-L882.
61. Kaser, M. R.; Skouteris, G. G., *Peptides (N. Y., NY, U. S.)* **1997**, *18* (9), 1441-4.
62. Bridges, J. P.; Wert, S. E.; Nogee, L. M.; Weaver, T. E., *J. Biol. Chem.* **2003**, *278* (52), 52739-52746.
63. Baoukina, S.; Monticelli, L.; Amrein, M.; Tieleman, D. P., *Biophys. J.* **2007**, *93* (11), 3775-3782.
64. Schurch, S.; Green, F. H. Y.; Bachofen, H., *Biochim. Biophys. Acta, Mol. Basis Dis.* **1998**, *1408* (2-3), 180-202.
65. Grigoriev, D. O.; Kragel, J.; Akentiev, A. V.; Noskov, B. A.; Miller, R.; Pison, U., *Biophys. Chem.* **2003**, *104* (3), 633-42.
66. Beers, M. F.; Mulugeta, S., *Annu. Rev. Physiol.* **2005**, *67*, 663-696.
67. Im Hof, V.; Gehr, P.; Gerber, V.; Lee, M. M.; Schurch, S., *Respir. Physiol.* **1997**, *109* (1), 81-93.
68. Geiser, M.; Schurch, S.; Gehr, P., *J. Appl. Physiol.* **2003**, *94* (5), 1793-801.
69. Kretzschmar, G.; Li, J.; Miller, R.; Motschmann, H.; Moehwald, H., *Colloids Surf., A* **1996**, *114* (Collection of Papers presented at the Workshop "Bubble and Drop 95", 1995), 277-285.
70. Krägel, J.; Li, J. B.; Miller, R.; Bree, M.; Kretzschmar, G.; Möhwald, H., *Colloid Polym. Sci.* **1996**, *274* (12), 1183-1187.
71. Wüstneck, R.; Wüstneck, N.; Grigoriev, D. O.; Pison, U.; Miller, R., *Colloids Surf., B* **1999**, *15* (3,4), 275-288.

72. Wüstneck, R.; Wüstneck, N.; Moser, B.; Karageorgieva, V.; Pison, U., *Langmuir* **2002**, *18* (4), 1119-1124.
73. Wüstneck, R.; Wüstneck, N.; Moser, B.; Pison, U., *Langmuir* **2002**, *18* (4), 1125-1130.
74. Wüstneck, N.; Wüstneck, R.; Fainerman, V. B.; Miller, R.; Pison, U., *Colloids Surf., B* **2001**, *21* (1-3), 191-205.
75. Domènech, Ò.; Sanz, F.; Montero, M. T.; Hernández-Borrell, J., *Biochim. Biophys. Acta* **2006**, *1758* (2), 213-221.
76. Notter, R. H.; Wang, Z.; Egan, E. A.; Holm, B. A., *Chem. Phys. Lipids* **2002**, *114* (1), 21-34.
77. Yan, W.; Biswas, S. C.; Laderas, T. G.; Hall, S. B., *J. Appl. Physiol.* **2007**, *102* (5), 1739-1745.
78. Krägel, J.; Kretzschmar, G.; Li, J. B.; Loglio, G.; Miller, R.; Möhwald, H., *Thin Solid Films* **1996**, *284-285*, 361-364.
79. Saulnier, P.; Boury, F.; Malzert, A.; Heurtault, B.; Ivanova, T.; Cagna, A.; Panaïeotov, I.; Proust, J. E., *Langmuir* **2001**, *17* (26), 8104-8111.
80. Wüstneck, R.; Perez-Gil, J.; Wüstneck, N.; Cruz, A.; Fainerman, V. B.; Pison, U., *Adv. Colloid Interface Sci.* **2005**, *117* (1-3), 33-58.
81. Kanno, S.; Furuyama, A.; Hirano, S., *Arch. Toxicol.* **2008**, *82* (11), 841-850.
82. Brown, N. J.; Johansson, J.; Barron, A. E., *Acc. Chem. Res.* **2008**, *41* (10), 1409-1417.

83. Ganguly, S.; Moolchandani, V.; Roche, J. A.; Shapiro, P. S.; Somaraju, S.; Eddington, N. D.; Dalby, R. N., *J. Aerosol Med. Pulm. Drug Delivery* **2008**, *21* (4), 343-350.
84. Erickson, B.; DiMaggio, S. C.; Mullen, D. G.; Kelly, C. V.; Leroueil, P. R.; Berry, S. A.; Baker, J. R.; Orr, B. G.; Banaszak Holl, M. M., *Langmuir* **2008**, *24* (19), 11003-11008.
85. Wu, C. W.; Seurnyck, S. L.; Lee, K. Y. C.; Barron, A. E., *Chem. Biol.* **2003**, *10* (11), 1057-1063.
86. Miller, R.; Wüstneck, R.; Krägel, J.; Kretschmar, G., *Colloids Surf., A* **1996**, *111* (1/2), 75-118.
87. Scherphof, G. L., *Phospholipids Handbook* **1993**, 777-800.
88. Vrănceanu, M.; Winkler, K.; Nirschl, H.; Leneweit, G., *Biophys. J.* **2008**, *94* (10), 3924-34.
89. Li, J. B.; Miller, R.; Vollhardt, D.; Weidemann, G.; Möhwald, H., *Colloid Polym. Sci.* **1996**, *274* (10), 995-999.
90. Saad, S. M. I.; Policova, Z.; Acosta, E. J.; Neumann, A. W., *Langmuir* **2008**, *24* (19), 10843-10850.
91. Prenner, E.; Honsek, G.; Hönig, D.; Möbius, D.; Lohner, K., *Chem. Phys. Lipids* **2007**, *145* (2), 106-118.
92. Rodriguez Nino Maria, R.; Caro Ana, L.; Rodriguez Patino Juan, M., *Colloids Surf., B* **2009**, *69* (1), 15-25.
93. Wüstneck, R.; Reiche, J.; Forster, S., *Thin Solid Films* **1997**, *307* (1,2), 100-105.

94. Hidalgo, A. A.; Tabak, M.; Oliveira, O. N., *Chem. Phys. Lipids* **2005**, *134* (2), 97-108.
95. Maltseva, E.; Shapovalov, V. L.; Möhwald, H.; Brezesinski, G., *J. Phys. Chem. B* **2006**, *110* (2), 919-926.
96. Zhang, Y.-P.; Lewis, R. N. A. H.; McElhaney, R. N., *Biophys. J.* **1997**, *72* (2, Pt. 1), 779-793.
97. Dicko, A.; Bourque, H.; Pezolet, M., *Chem. Phys. Lipids* **1998**, *96* (1-2), 125-139.
98. Goni, F. M.; Alonso, A., *Prog. Lipid Res.* **1999**, *38* (1), 1-48.
99. Dyck, M.; Krüger, P.; Lösche, M., *Phys. Chem. Chem. Phys.* **2005**, *7* (1), 150-6.
100. Pimthon, J.; Willumeit, R.; Lendlein, A.; Hofmann, D., *J. Mol. Struct.* **2009**, *921* (1-3), 38-50.
101. Hübner, W.; Blume, A., *Chem. Phys. Lipids* **1998**, *96* (1-2), 99-123.
102. Bruni, R., *Am. J. Physiol. Lung Cell Mol. Physiol.* **2002**, *283* (5), L894-6.
103. Takamoto, D. Y.; Lipp, M. M.; Von Nahmen, A.; Lee, K. Y. C.; Waring, A. J.; Zasadzinski, J. A., *Biophys. J.* **2001**, *81* (1), 153-169.
104. Wang, Z.; Baatz, J. E.; Holm, B. A.; Notter, R. H., *Am. J. Physiol.* **2002**, *283* (5, Pt. 1), L897-L906.
105. Pattle, R. E., *Nature (London, U. K.)* **1955**, *175* (4469), 1125-6.
106. Derwent, R. G.; Simmonds, P. G.; Manning, A. J.; Spain, T. G., *Atmos. Environ.* **2007**, *41* (39), 9091-9098.
107. Veldhuizen, E. J. A.; Batenburg, J. J.; Van Golde, L. M. G.; Haagsman, H. P., *Biophys. J.* **2000**, *79* (6), 3164-3171.
108. Zahardis, J.; Petrucci, G. A., *Atmos. Chem. Phys.* **2007**, *7*, 1237-1274.

109. Neeb, P.; Sauer, F.; Horie, O.; Moortgat, G. K., *Atmos. Environ.* **1997**, *31* (15), 1417-1423.
110. Wadia, Y.; Tobias, D. J.; Stafford, R.; Finlayson-Pitts, B. J., *Langmuir* **2000**, *16* (24), 9321-9330.
111. McConlogue, C. W.; Vanderlick, T. K., *Langmuir* **1998**, *14* (22), 6556-6562.
112. López-Montero, I.; Arriaga, L. R.; Monroy, F.; Rivas, G.; Tarazona, P.; Vélez, M., *Langmuir* **2008**, *24* (8), 4065-4076.
113. Li, J. B.; Kretzschmar, G.; Miller, R.; Möhwald, H., *Colloids Surf., A* **1999**, *149* (1-3), 491-497.
114. Mansour, H. M.; Damodaran, S.; Zografi, G., *Mol. Pharmaceutics* **2008**, *5* (5), 681-695.
115. Agency, U. S. E. P. AIRNow.gov. (accessed 2009 12 21).
116. Berg, J.; Tymoczko, J.; Stryer, L., *Biochemistry*. 5th ed.; Julet, M.: New York, 2002.
117. Manzanares, D.; Rodriguez-Capote, K.; Liu, S.; Haines, T.; Ramos, Y.; Zhao, L.; Doherty-Kirby, A.; Lajoie, G.; Possmayer, F., *Biochemistry* **2007**, *46* (18), 5604-5615.
118. Rodríguez-Capote, K.; Manzanares, D.; Haines, T.; Possmayer, F., *Biophys. J.* **2006**, *90* (8), 2808-2821.
119. Ma, G.; Allen Heather, C., *Langmuir* **2006**, *22* (26), 11267-74.

Appendix I

Equations used for calculation of viscoelastic parameters^{14, 16, 17}.

$$E(i\omega) = \frac{F\{\delta\sigma(t)\}}{F\{\delta \ln A(t)\}} \quad \text{Equation (A1)}$$

F: denotes the Fourier transform operator

ω : circular frequency ($= 2\pi f$)

t: time (s)

$\delta\sigma(t)$: surface tension response (mN m^{-1})

$\delta \ln A(t)$: variation of surface area (m^2)

$$E(i\omega) = E'(\omega) + iE''(\omega) = |E| \exp(i\theta) \quad \text{Equation (A2)}$$

$$|E| = \sqrt{E'^2 + E''^2}, \tan \theta = \frac{E''}{E'} \quad \text{Equation (A3)}$$

θ : phase angle between harmonic oscillations

$$\varepsilon(\omega) = E'(\omega) \quad \text{Equation (A4)}$$

ε : elasticity (mN m^{-1})

$$\eta(\omega) = \frac{E''(\omega)}{\omega} = \frac{\varepsilon \tan \theta}{\omega} \quad \text{Equation (A5)}$$

η : viscosity (mN s m^{-1})

Appendix II

ESI-MS data for oxidized POPG.

Molecule	Mass (m/z)
1-palmitoyl-2-oleyl-phosphatidylglycerol	747.6
1-palmitoyl-2-(9-oxononanoyl)phosphatidylglycerol	637.4
1-palmitoyl-2-(9-carboxynonanoyl)phosphatidylglycerol	653.7
1-palmitoyl-2-(9-hydroxy-9-hydroperoxynonanoyl)phosphatidylglycerol	669.4

